INVESTIGATING THE HIGH-TEMPERATURE (100 °C – 200 °C) DISSOLUTION AND SULFIDATION OF As_2O_3 STORED AT THE GIANT MINE, NWT, CANADA

EVELYN TENNANT

Thesis submitted in partial fulfillment of the requirements for the
Master's Degree of Science

Department of Earth and Environmental Sciences
Faculty of Science
University of Ottawa

Abstract

The Giant Mine near Yellowknife, NWT generated 237 000 tonnes of arsenic-trioxide (As_2O_3)-rich dust as a by-product of gold mining during its years of operation (1948 – 2004). Arsenic trioxide is a relatively soluble form of arsenic (As) and is currently stored in the mine, posing a threat of contamination to the adjacent Great Slave Lake. This research investigates the potential for permanent remediation of the As_2O_3 using sulfidation to transform it to arsenic trisulfide (As_2S_3).

Knowing that aqueous As_2O_3 readily reacts with sulfide (Ostermeyer, 2021), it was determined that the most practical and effective method to achieve sulfidation of the Giant Mine dust is to first dissolve the As_2O_3 and then conduct the reaction with sulfide. The optimal conditions at which to dissolve As_2O_3 were investigated. The solubility and dissolution rate in water were shown to increase with temperature, with solubility increasing from 185.7 g As_2O_3/kg water at 140 ^oC to 250.6 g As_2O_3/kg water at 180 ^oC. Qualitative demonstrations of the rate of dissolution show that ≥ 90 % of the As_2O_3 dissolved within 5 minutes at 140 ^oC, and 4 minutes at 180 ^oC; previous research indicates that time to equilibrium is > 24 hours at 60 ^oC (CANMET, 2000). Reaction of Giant-Mine material in water at elevated temperatures (140 ^oC – 200 ^oC) for 10 to 30 minutes consistently resulted in dissolution of approximately 80 wt. % of the initial solid-phase As concentrations, representing almost all the As_2O_3, yielding undissolved residues (≈ 40 wt. % of initial mass). The persistence of As in these residues is likely due to it being hosted in As_2O_3 - Sb_2O_3 solid solutions and low-solubility Fe-oxide phases in the initial sample (CANMET, 2000; Poirier, 2004).

Résumé

La mine Giant, située près de Yellowknife dans les Territoires du Nord-Ouest, a généré 237 000 tonnes de poussière riche en trioxyde de diarsenic (As_2O_3) en tant que sous-produit de l'extraction de l'or au cours de ses années d'exploitation (1948 - 2004). Le trioxyde de diarsenic est une forme relativement soluble d'arsenic (As) et est actuellement entreposé dans la mine, ce qui représente un risque de contamination pour le Grand lac des Esclaves adjacent. Cette étude examine le potentiel de remédiation permanente de l'As_2O_3 en utilisant la sulfuration pour le transformer en trisulfure d'arsenic (As_2S_3).

Sachant que l'As_2O_3 aqueux réagit facilement avec le sulfure (Ostermeyer, 2021), il a été déterminé que la méthode la plus pratique et la plus efficace pour réaliser la sulfuration de la poussière de la mine Giant est de dissoudre d'abord l'As_2O_3, puis effectuer la réaction avec le sulfure par la suite. Les conditions optimales de dissolution de l'As_2O_3 ont été examinées. Il a été démontré que la solubilité et la vitesse de dissolution dans l'eau augmentent avec la température, la solubilité passant de 185,7 g As_2O_3/kg d'eau à 140 ^oC, à 250,6 g As_2O_3/kg d'eau à 180 ^oC. Les démonstrations qualitatives de la vitesse de dissolution montrent que ≥ 90 % de l'As_2O_3 s'est dissous en 5 minutes à 140 ^oC, et en 4 minutes à 180 ^oC, alors que des études antérieures indiquent que le temps nécessaire pour atteindre l'équilibre est de > 24 heures à 60 ^oC (CANMET, 2000). La réaction des matériaux de la mine Giant dans l'eau à des températures élevées (140 ^oC - 200 ^oC) pendant 10 à 30 minutes a systématiquement entraîné la dissolution d'environ 80 % en poids des concentrations initiales d'As en phase solide, représentant presque tout l'As_2O_3, ce qui a donné des résidus non dissous (≈ 40 % en poids de la masse initiale). La persistance de l'As dans ces résidus est probablement due au fait qu'il est retrouvé dans des solutions solides As_2O_3 - Sb_2O_3 et dans des phases d'oxyde de fer peu solubles de l'échantillon initial (CANMET, 2000 ; Poirier, 2004).

Acknowledgments

I would first like to thank my supervisor, Dr. Tom Al, for his invaluable support throughout this process. I cannot express enough how appreciative I am of his contribution to my knowledge in the field of geochemistry, my professional development, and for his overall support.

I would also like to thank all the support staff at the University of Ottawa whose assistance was critical in the development of my research. This includes, but is not limited to, Glenn Poirier, Alain Mauviel, Jeffrey Ovens, Nimal De Silva, and Smita Mohanty.

I would like to thank all of Tom's research team and the uOttawa graduate students for their support as colleagues and friends. Special thanks to Magda, Hannah, Nikki, Alex, Guadalupe, and Chris. I especially want to thank Carla; her support and friendship will not be forgotten, and she will be greatly missed.

Thank you, Kevin, for pushing me to be my best self.

Finally, thank you to all my family and friends for their endless support and encouragement. I will walk away from this experience with more knowledge, experience, and resilience than I could have hoped for, and I have everyone mentioned above to thank.

A special thank you goes out to the Giant Mine Oversight Board and the Canadian Natural Science and Engineering Research Council (NSERC) Towards Environmentally Responsible Resource Extraction Network (TERRE-NET), for funding which supported this research. Additional funding was provided by NSERC (Grant number 712210101627).

Table of Contents

List of Figures

List of Tables

1. Introduction

1.1. Giant Mine history

The Giant Mine is located five kilometres north of Yellowknife, NWT, adjacent to Great Slave Lake and near the Indigenous communities of Ndilo and Dettah (Figure 1-1). It produced over seven million troy ounces of gold during its years of operation (1948 – 2004) (Jamieson, 2014). The gold-bearing arsenopyrite- and pyrite-rich ore required a roasting step prior to gold recovery using cyanidation. The roasting process was operated at approximately 500 ^{o}C, and arsenic-rich gases released by roasting were condensed, with the arsenic captured as As_2O_3-rich dust. Approximately 237 000 tonnes of the dust were collected in a baghouse and stored in mined-out stopes and purpose-built chambers in the mine. If the mine is allowed to flood, dissolution of the As_2O_3-rich dust presents a risk of arsenic contamination to nearby water bodies, primarily Great Slave Lake. According to CBC (Cohen), the Giant Mine clean up, including the As_2O_3-rich dust is currently the most expensive ($4.38 B) project in Canada's Northern Abandoned Mine Reclamation Program.

1.2. Giant Mine As_2O_3 remediation

1.2.1. Risk

If an effective remedial method is not implemented, there is risk of arsenic contamination to the water bodies surrounding the mine. Seepage from the As_2O_3 chambers has been determined to be the dominant source of arsenic in mine waters, with the maximum measured concentration being 4.21 g/L from seepage through fractured rock near one of the chambers (Clark, 2001).

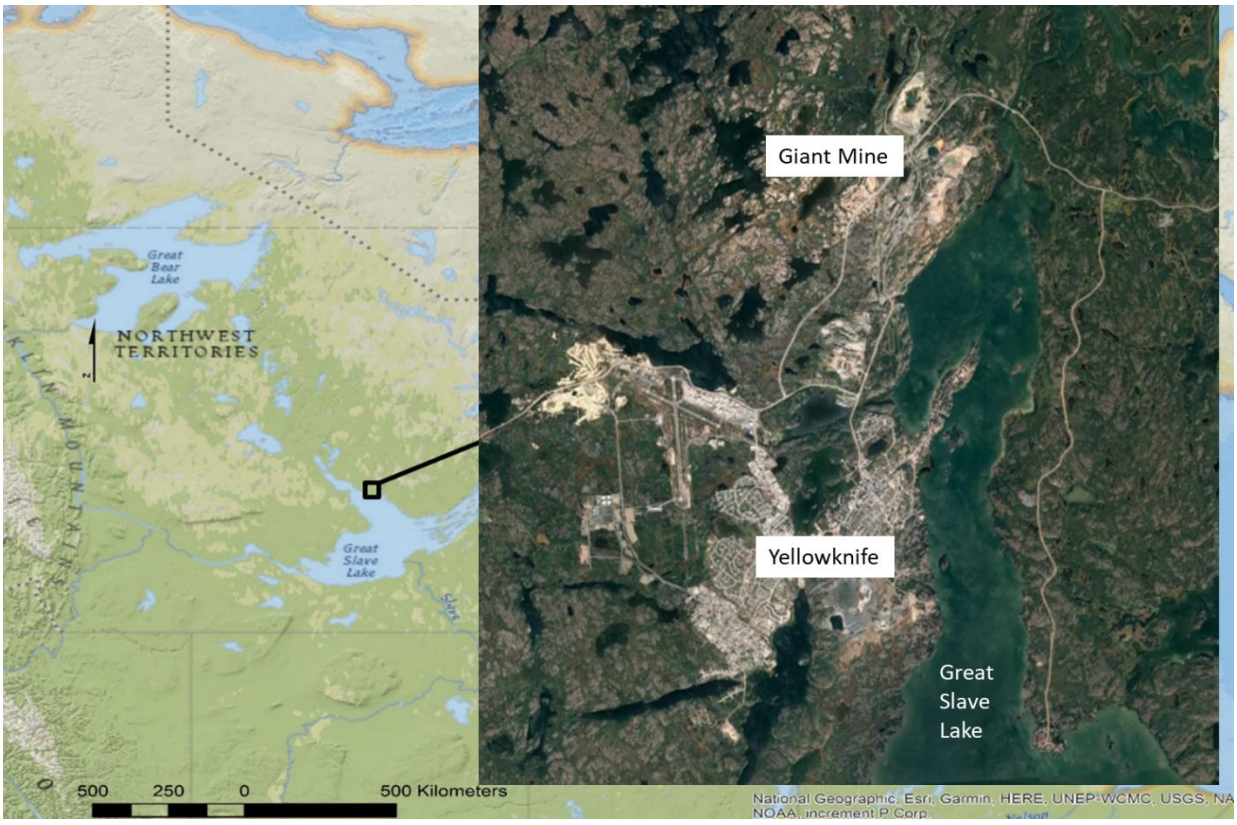

Figure 1-1: Location of Giant Mine.

The arsenic-filled chambers within the Giant Mine reach a depth of approximately 410 meters, and the groundwater is currently being pumped to maintain the water table at a depth of approximately 425 meters (SRK 2002a; SRK 2002b). The regional pattern of groundwater flow is toward Great Slave Lake. Therefore, if pumping is not maintained, the water table would rise above the level of the As_2O_3 chambers and contaminated groundwater would flow into the lake.

1.1.1. Current remediation plan

There is currently a remediation plan in place that involves freezing the ground surrounding the stored As_2O_3 using thermosyphon technology (SRK & SENES, 2007), generally referred to as the frozen-block method. The thermosyphons act as passive heat pumps, maintaining a frozen condition in and around the chambers (SRK & SENES, 2007). If the As_2O_3 is in a frozen state, the mine can be reflooded with a reduced risk of arsenic release to the environment. The success of this remediation plan is contingent on the functionality of the thermosyphons and duration of funding for operation and maintenance.

1.2. Project concept

This research project investigates a remediation alternative for the As_2O_3-rich dust stored at the Giant Mine. To minimize risk of contamination to the surrounding environment, a remediation method should provide a permanent solution. The goal of this research is to convert the As_2O_3-rich dust into a less soluble and bioavailable form. Conversion of As_2O_3 into a stable alternative would reduce the reliance on the frozen block strategy which is susceptible to technical malfunctions and reliant on constant funding into the future.

This project investigates the stabilization of As_2O_3 by sulfidation. Conversion of As_2O_3 to a stable (low-solubility) sulfide form is examined through the net reaction:

$$As_2O_{3\,(s)} + 3H_2S_{\,(g)} \rightarrow As_2S_{3\,(s)} + 3H_2O_{\,(l)} \quad [1]$$

In this net reaction, "As_2S_3" can represent either the mineral orpiment, or an amorphous form.

The process of remediation through sulfidation would occur *ex situ*, involving the removal of the As_2O_3 from storage chambers, followed by the injection of the As_2S_3 product/slurry deep into the mine for storage (~600 m). Ultimately, the method must be implemented at the industrial scale, and this must be considered when developing research objectives to ensure method feasibility, material availability, and cost efficiency.

1.3. Literature review

1.3.1. Properties of As_2O_3

Arsenic trioxide enters the environment through natural processes, such as volcanic eruptions and the weathering of arsenic-bearing minerals, however it is mostly produced as an oxidation product of the roasting of arsenic-bearing ore minerals (O'Day, 2006). The compound As_2O_3 is particularly problematic due to its relatively high solubility and bioavailability compared to other arsenic compounds. Previous research has shown that As_2O_3 is one of the most bioavailable forms of arsenic (Jamieson, 2014; Plumlee and Morman, 2011).

Aqueous arsenic speciation

Aqueous As occurs primarily as the oxy-anions arsenite ($As^{III}O_3^{3-}$) and arsenate ($As^{V}O_4^{3-}$) and their hydrolysis products (O'Day, 2006). The speciation of aqueous As with respect to pH and Eh is displayed in Figure 1-2. Arsenite, the soluble product of As_2O_3 dissolution, occurs under relatively reducing conditions over a wide range of pH values (~0-9) (Nordstrom & Archer, 2002) and is the most soluble form of arsenic.

Arsenic trioxide solubility

The solubility of As_2O_3 in water has previously been determined to systematically increase with temperature. Solubility was determined by CANMET (2000) to range from approximately 20 g As_2O_3/kg water at 25 ^oC to 83 g As_2O_3/kg water at 100 ^oC. A compilation of solubility values from multiple studies, ranging from 0 ^oC to 250 ^oC was made by Pokrovski et al. (1996). Measured solubilities ranged from 12.1 g As_2O_3/kg water at 0 ^oC to 1570 ± 140 g As_2O_3/kg water 250 ^oC; during these experiments, it was found that arsenolite[1] (cubic As_2O_3) transformed to claudetite (monoclinic As_2O_3) at temperatures greater than 150^oC. A linear trendline (R^2=0.9718) shown in Figure 1-3 fits the solubility measurements compiled by Pokrovski et al. (1996) and those measured by CANMET (2000).

[1] For remainder of this document, As_2O_3 will describe arsenolite unless otherwise specified.

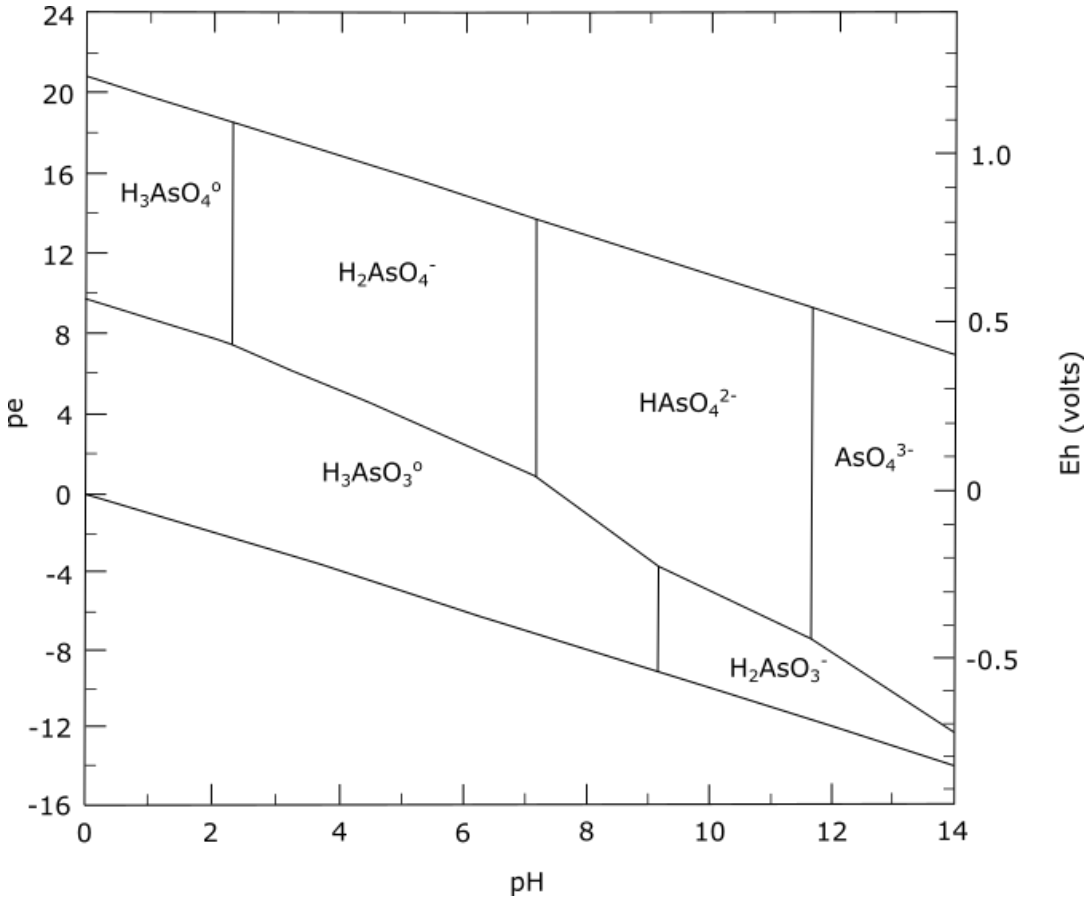

Figure 1-2: Aqueous arsenic speciation, at equilibrium, at 298.15°K and 1 atmospheric pressure (modified from Nordstrom and Archer, 2002).

Arsenic trioxide dissolution rate

While the data describing the dissolution and precipitation rates for As_2O_3 are sparse, the rate of reagent-grade As_2O_3 dissolution was investigated by CANMET (2000) at 25 °C and 60 °C. In these experiments, reagent grade As_2O_3 was stirred for 3 days at 25 °C, and > 24 hours at 60 °C to reach equilibrium.

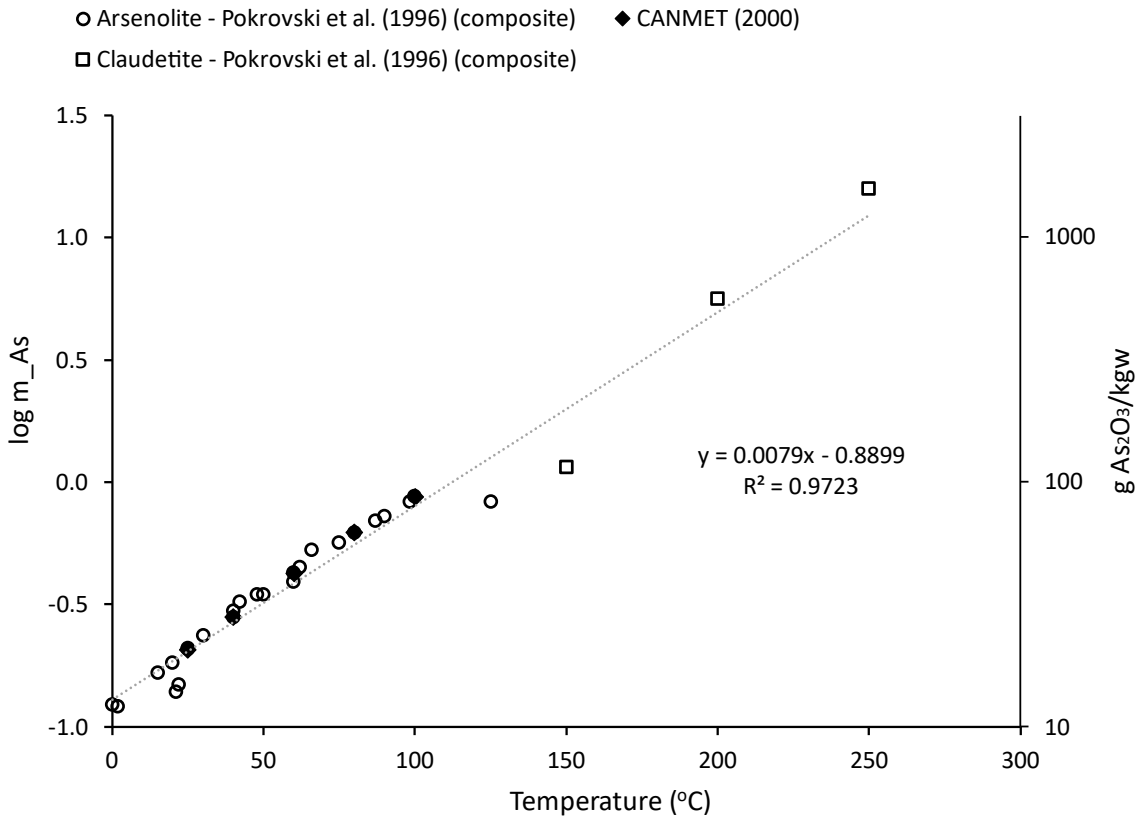

Figure 1-3: Compilation of arsenic trioxide solubilities determined in previous research (Anderson and Story, 1923; Baes and Mesmer, 1976; CANMET, 2000; Linke, 1958; Pokrovski et al., 1996; Stranski et al. 1958).

1.3.2. Properties of As_2S_3

The sulfidation of As (III) solutions has been investigated by Ostermeyer et al. (2021); sulfide was introduced to acidic (pH=2) metallurgical wastewater at various S:As molar ratios. The results indicate that at a molar S:As ratio of 5, near complete removal of As from a 5 g As/L solution occurred within one minute.

For anoxic dissolution of As_2S_3, As (III) is the predominant dissolved arsenic species (Equation 2; Eary 1992; Floroiu et al. 2004). Although, it was found by Eary (1992) and Webster (1990) that Equation 2 occurs in sulfide-deficient solutions, and that the thioarsenite species $H_2As_3S_6^-$ is present in acidic sulfide-rich solutions (> 10^{-2} molal) and may be an equal contributor to overall As solubility [Equation 3].

$$0.5As_2S_3\,(s) + 3H_2O \leftrightarrow H_3AsO_3 + 1.5H_2S \qquad [2]$$

$$1.5As_2S_3\,(s) + 1.5HS^- + 0.5H^+ \leftrightarrow H_2As_3S_6^- \quad [3]$$

An increase in As_2S_3 solubility was reported in sulfide-rich solutions, where S:As molar ratios exceed 4, at pH 4 (Eary, 1992; Webster, 1990; Wilkin et al., 2003). However, experiments conducted with metallurgical wastewaters did not report an increase in As_2S_3 dissolution up to S:As molar ratios of 20 (Ostermeyer, 2021); it was suggested that this contradiction could be explained by destabilization of soluble As-S complexes at low pH (< 2) in the metallurgical wastewater.

The solubility of As_2S_3 is primarily dependent on pH and redox conditions (Nordstrom & Archer, 2002). Its solubility at various pH conditions has been investigated in detail (Eary 1992; Floroiu et al. 2004; Mirazimi 2020), with the conclusion that solubility and dissolution rates increase above pH 5.5. Below pH 5.5, solubility of As_2S_3 is independent of pH.

Amorphous $As_2S_{3\,(am)}$ is 10 to 16 times more soluble than orpiment (Eary 1992; Mironova et al. 1984). Dissolution of $As_2S_{3\,(am)}$ between pH 2 and 5 yielded maximum As (III) concentrations of ≈ 0.001 g As_2S_3/ kg water 25 ^oC (Floroiu et al., 2004). Therefore, despite its higher solubility compared to orpiment, the solubility of $As_2S_{3\,(am)}$ is a factor of approximately 20,000 lower than As_2O_3 at 25 ^oC (20 g As_2O_3/ kg water) in the pH range 2 to 5.

Arsenic trisulfide solubility (Mirazimi, 2020) and dissolution rate (Lengke & Tempel, 2001) increase in the presence of dissolved O_2 (DO). Oxidative dissolution of As_2S_3 occurs according to the reaction shown in Equation 4, releasing arsenous acid into solution. The rate expression (Equation 5) for dissolution of $As_2S_{3(am)}$ in the presence of DO is provided by Lengke & Tempel (2001).

$$As_2S_3 + 6O_2 + 6H_2O \rightarrow 2H_3AsO_3 + 3SO_4^{2-} + 6H^+ \quad [4]$$

$$R(As) = 10^{-16.77}\,[DO]^{0.42}\,[H^+]^{-1.26} \quad [5]$$

1.3.3. Storage of As_2S_3 at the Giant Mine

The elevated solubility and dissolution rate of As_2S_3 in the presence of DO necessitates an anoxic storage environment. If an As_2S_3 product is injected deep into the mine, an anoxic environment can be ensured for several reasons:

1. The groundwater at the 600 m depth in the Giant Mine is a brine with NaCl concentrations of 5 – 6 g/L (Clark, 2001). The relatively high density of the brine compared to the shallow groundwater would ensure isolation from the shallow, oxygenated flow system.
2. The Giant Mine property lies within the Yellowknife Greenstone belt, consisting of Archaean metavolcanic and metasedimentary rocks which are iron-rich (Jamieson, 2014). Reactions resulting from contact between Fe-rich minerals and the groundwater are expected to consume any available DO, effectively buffering the redox conditions in an anoxic state; as redox conditions have often been demonstrated to be controlled by water-rock interactions (e.g. Lichtner & Waber, 1992, Grenthe et al., 1992).

1.3.4. Giant Mine As_2O_3-rich dust characteristics

The composition and grain size of the Giant Mine dust is heterogeneous according to SRK (2004) wherein they provide a list of dates when the various chambers and stopes were filled, the dust mass, and the arsenic concentrations in each chamber (Table 1-1; Table 1-2). Arsenic concentrations are higher in chambers filled after 1963 because of improvements made to the efficiency of the roaster and the electrostatic precipitator circuits (SRK, 2004). The grain size is reported to range from 10 µm to 55 µm; 88.5% of the dust is less than 45 µm (SRK, 2004).

Table 1-1: Quantity and filling dates for Giant Mine chambers and stopes

Chamber/Stope	Dust Inventory (dry tonnes)	Primary Filling Period
B230	2835	1951 – 1952
B233	11 426	1952 – 1956
B234	12 048	1956 – 1958
B235/236	32 945	1958 – 1962
B208	29 364	1962 – 1964
B212/213/214	59 289	1965 – 1973
C212	16 946	1973 – 1982
#9	18 394	1976 – 1980
#10	9569	1982 – 1985
#11	5860	1986 – 1988
#12	26 243	1988 – 1994
#14	12 257	1995 – 1999
Total	237 343	1951 – 1999

Note. Modified from SRK (2004)

Table 1-2: Summary of elemental concentrations for Giant Mine dust samples (=8) (SGS Lakefield Research, 2004)

Element	Average (mg/kg)	Median (mg/kg)	RSD (wt. %)
Ag	12	7.5	97
Al	11 000	8 500	49
Ba	28	25	38
Be	0	0.1	46
Ca	5 200	4 400	53
Cd	9.3	12.5	44
Co	41	28	71
Cr	33	27	52
Cu	280	230	76
Fe	44 000	24 000	94
K	3000	2400	47
Mg	3600	3300	58
Mn	150	115	53
Na	524	465	55
Ni	81	52	74
Pb	1200	680	100
Sb	10 000	9600	61
Sr	5600	7.1	260
Ti	770	560	77
V	41	34	46
Y	1.3	1	37
Zn	591	360	99
As	590 000	610 000	15

Giant Mine dust composition and mineralogy

Geochemical analyses were conducted on eight Giant Mine dust samples (Table 1-2) (SGS Lakefield Research, 2004). The most abundant elements are As, Fe, Sb, and Al, but the range of values for each is variable with relative standard deviations ranging from 15% to 94%. Dust obtained from roasting low-grade ore contains relatively high impurity contents (Fe, Sb) and lower As concentrations; notably, sample B233-P9 contains the lowest As concentration (39.5%) and the highest Fe and Sb concentrations (15% and 1.8% respectively) of the eight chamber samples reported by SGS Lakefield Research (2004) (Appendix A, Table 1).

On the basis of mineralogical analyses conducted on eight samples by CANMET (2000) and Poirier (2004), it was concluded that the mineralogy is broadly similar, and only varies in the relative quantities of As_2O_3 and accessory phases. The mineralogy of dust samples from two storage chambers (B233-P9 and C212-2) is summarized in Table 1-3. The material in these chambers was produced before (B233-P9) and after (C212-2) improvements were made to the roaster and electrostatic precipitator circuits. While As_2O_3 is the dominant phase in both samples, hematite is also a major phase in the 'older' dust.

The dominant host for As in the samples, investigated by CANMET (2000) and Poirier (2004), was As_2O_3 - Sb_2O_3 solid solutions, with the Sb content of the solid solutions ranging from 0 to 47 % in the samples investigated by CANMET (2000). Minor hosts include an As-bearing iron oxide phase and iron arsenate.

Table 1-3: Comparative mineralogy between and 'old' and 'new' Giant Mine dust, identified with X-Ray Diffraction (XRD)

Sample	Identified Minerals	
	Major	Accessory
B233-P9	As_2O_3, hematite	muscovite, clinochlore, pyrite, gypsum, quartz
C212-2	As_2O_3	clinochlore, muscovite, gypsum, quartz

Modified from Poirier (2004)

Giant Mine dust dissolution characteristics

Measurements on four samples of Giant Mine dust (CANMET, 2000) indicate that the solubility is approximately half that of reagent grade As_2O_3. The samples consisted of composites made in 1997 and 1998, as well as samples from chamber 212 and chamber 236. Arsenic concentrations were measured after the dust was stirred in water for three days at temperatures ranging from 20 ^oC to 100 ^oC. The As concentrations from samples with the highest (B236) and lowest (B212) As_2O_3 solubility are plotted in comparison to reagent-grade As_2O_3 in Figure 1-4. The study conducted by CANMET (2000) detected a correlation between an increase in Sb concentration within the Giant Mine dust samples and decreased As_2O_3 solubility. The range of Sb concentrations in the four analyzed samples was 0.30 to 2.13 %.

The dissolution rate of the dust was investigated on a single sample, from Giant Mine chamber 212. Eight hours were required to reach a steady-state As_2O_3 concentration (35 g As_2O_3/ kg water) during a dissolution experiment at 95 ^oC (CANMET, 2000).

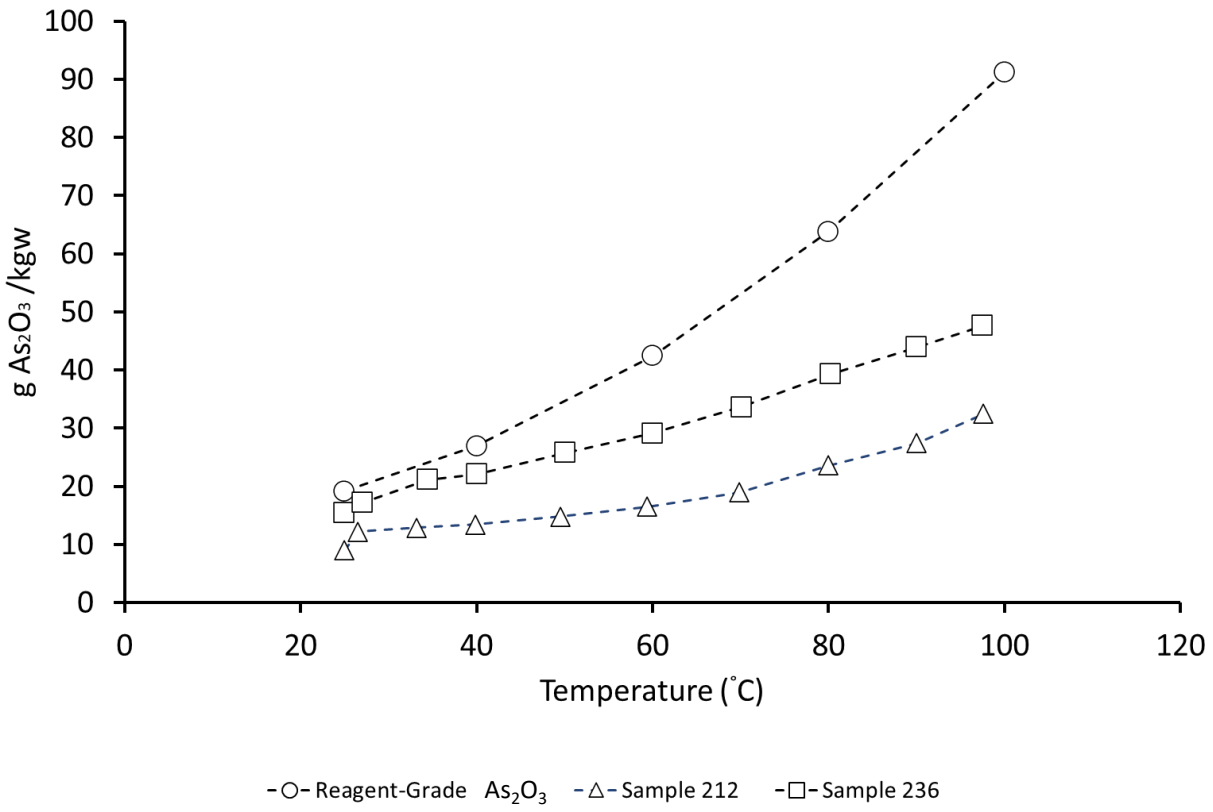

Figure 1-4: Comparison of the solubility of Giant Mine dust and reagent-grade As_2O_3.

1.4. Research objectives

The overall objective of this study is to explore methods to transform As_2O_3 to a less soluble sulfide form, with a focus on As_2S_3. The best route to achieving this objective was not known at the outset, but several possible approaches were considered which are represented by the following specific objectives.

Heterogeneous reaction:

- Conduct experiments to test the viability of directly transforming solid As_2O_3 to As_2S_3 using H_2S as a sulfide source.
- Characterize the solid reaction products to assess the extent of the reaction.

Homogeneous reaction:

- If the heterogeneous reaction approach is not successful, then it will be necessary to first dissolve the As_2O_3 and then react the As(III) with sulfide (S^{2-}) in a homogeneous aqueous solution. Experiments will be conducted to identify suitable methods for dissolving the As_2O_3 dust,

followed by sulfidation. Specifically, these experiments will determine the most practical and efficient method for As_2O_3 dissolution.

- Determine the solubility and dissolution rate of As_2O_3 at elevated temperatures (>100 °C).
- Using water at elevated temperatures (>100 °C), determine the optimal conditions (time, temperature) to dissolve As_2O_3 from the Giant Mine dust.
- Conduct geochemical and mineralogical characterization of the insoluble residue.

2. Materials and methodology

The sulfidation of As_2O_3 to As_2S_3 was investigated in two ways, as outlined in Figure 2-1: heterogeneous and homogenous reactions. The homogenous reaction requires that the As_2O_3 first be dissolved prior to the addition of sulfide, whereas in the heterogeneous reaction, sulfide is added to an As_2O_3 slurry. Both methods were first explored using pure, reagent-grade As_2O_3, and in the case of homogeneous reactions, this was followed by experiments using As_2O_3-rich waste from the Giant Mine.

2.1. Materials

Prior to use in experiments, reagent-grade As_2O_3 (99.5%, Alfa Aesar) was embedded in epoxy and imaged with Scanning Electron Microscopy (SEM) to assess the particle grain size. Experiments using the Giant Mine waste were conducted with archived material from sample B233-P9. This material was chosen for the experiments because it has the highest Sb content of all available archived material (18 000 mg/kg; SGS Lakefield Research, 2004). As a result, the As_2O_3 within this sample was expected to have the lowest solubility and therefore represent the most challenging endmember, among the available samples.

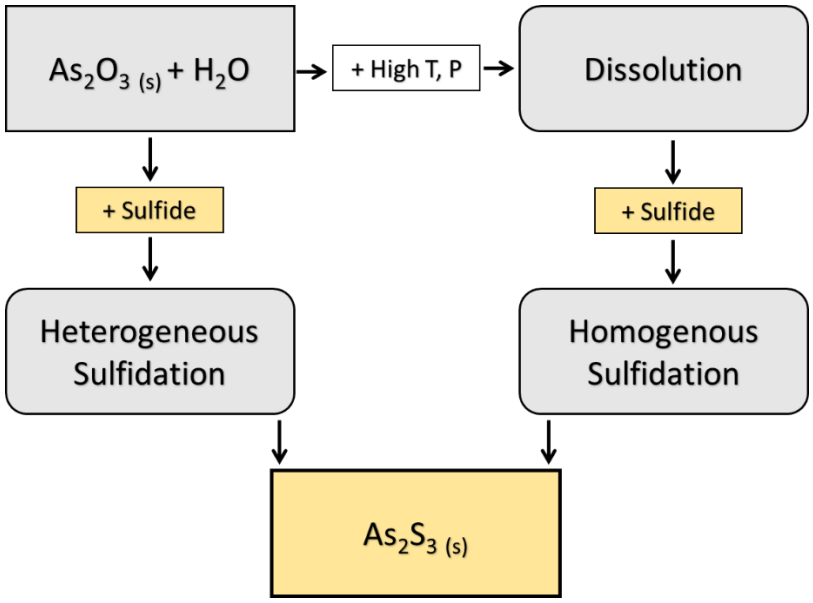

Figure 2-1: Flowchart outlining the proposed pathways to achieve sulfidation of As_2O_3 to form As_2S_3, where T represents temperature and P represents pressure.

Giant Mine sample B233-P9 consists of a mixture of large aggregates (Figure 2-2 A) and finer material (Figure 2-2 B). Both fractions of the sample are magnetic. Prior to conducting experiments with this material, the variability in chemical composition was assessed with 10 analytical replicates of the coarse aggregates and 5 replicates from the finer material. The material was crushed prior to being weighed into Savillex PTFE vials (≈ 30 mg each). The replicates were dissolved in 1 mL of concentrated aqua regia (3:1 molar HCl: HNO_3) at 90 ^oC for 24 hours with the vials capped. A solid residue remained within each vial, which was dried and prepared on a grain mount and analysed with Scanning Electron Microscopy and Energy Dispersive Spectroscopy (SEM-EDS). No As or Sb was detected in the undigested residue.

The digested samples were then diluted to 2% aqua regia with distilled water for analysis with Inductively-Coupled-Plasma Atomic-Emission Spectroscopy (ICP-OES).

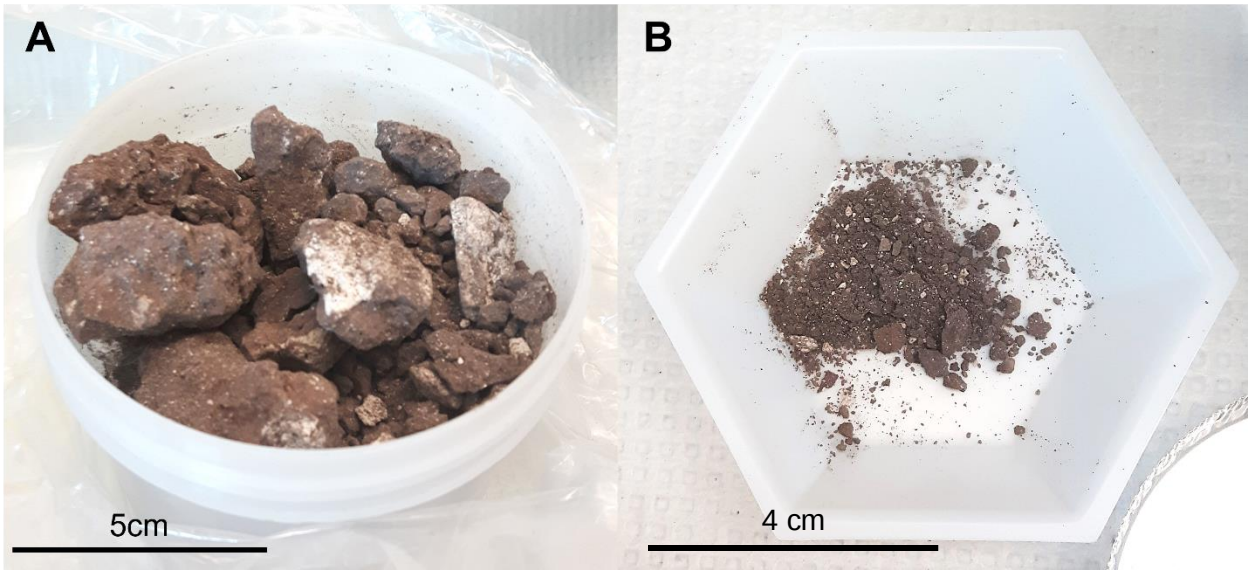

Figure 2-2: Giant Mine sample B233-P9 A: Coarse aggregates and B: Finer-grained material.

2.2. Heterogeneous As_2O_3 sulfidation

2.2.1. Modelling

Aqueous geochemical modelling was conducted with the equilibrium geochemical code, PHREEQC (WATEQ4F database; Parkhurst and Appelo, 2013) to simulate the reaction between H_2S and an aqueous slurry of As_2O_3 in water (input file: Appendix B, File 1), to test the thermodynamic viability of the reaction. Hematite (Fe_2O_3) (0.14 moles) and arsenolite (As_2O_3) (1 mole) were added as solid (equilibrium) phases, in concentrations similar to those in the Giant Mine dust, to a solution with a composition typical of groundwater (Table 2-1). Sulfide, in the form of H_2S was incrementally added to the solution to promote the precipitation of orpiment, or amorphous As_2S_3, from the slurry.

2.2.2. Experimental

The experimental setup for heterogeneous sulfidation experiments is displayed in Figure 2-3. Approximately 1 g of reagent-grade As_2O_3 was added to a 250-mL Pyrex® reaction vessel, which was sealed and purged with N_2 to remove atmospheric O_2. The vessel was then filled with 120 mL of deaerated distilled water which was acidified to a pH of 3 with deaerated HCl. After purging the entire system with N_2, H_2S gas (99%) was introduced to the reaction vessel through a gas dispersion tube at a pressure of slightly

greater than 1 atm. Once a steady stream of H_2S began to flow through the vessel, the experiment was run for two hours. Excess H_2S was collected into a beaker containing dissolved NaOH with a gas dispersion tube; the H_2S dissolved into the NaOH solution, preventing H_2S (g) from being released into the fume hood. After two hours, the solid reaction product was collected on a filter membrane (0.45 μm) and dried under N_2 and H_2 in an anaerobic chamber prior to further analysis.

Table 2-1: Initial concentrations used in PHREEQC model of homogenous As_2O_3 sulfidation

Solid Concentration (g/kg water)		Aqueous Concentration (mg/kg water)	
Hematite	7.985	Ca	15
Arsenolite	198	Mg	2
		Na	20
		K	0.5
		Fe	0.001
		HCO_3	25
		SO_4	30
		Cl	27

2.3. Homogeneous As_2O_3 sulfidation

The timing of As_2S_3 precipitation in a homogeneous aqueous solution upon the addition of acid was investigated qualitatively. The experiment involved gradual addition of acid to a solution containing As(III) and S^{2-} to force the system into a condition of saturation or super saturation with respect to As_2S_3. This would allow visual observation of precipitation of the yellow As_2S_3 precipitate. A Hach® digital titrator was used to add 1.6 N H_2SO_4 to a 35 mL solution containing dissolved As_2O_3 (20 g As_2O_3/L) and an excess (≈3025 mg S^{2-} /L) of $Na_2S{\cdot}9H_2O$. The pH was monitored potentiometrically throughout the experiment.

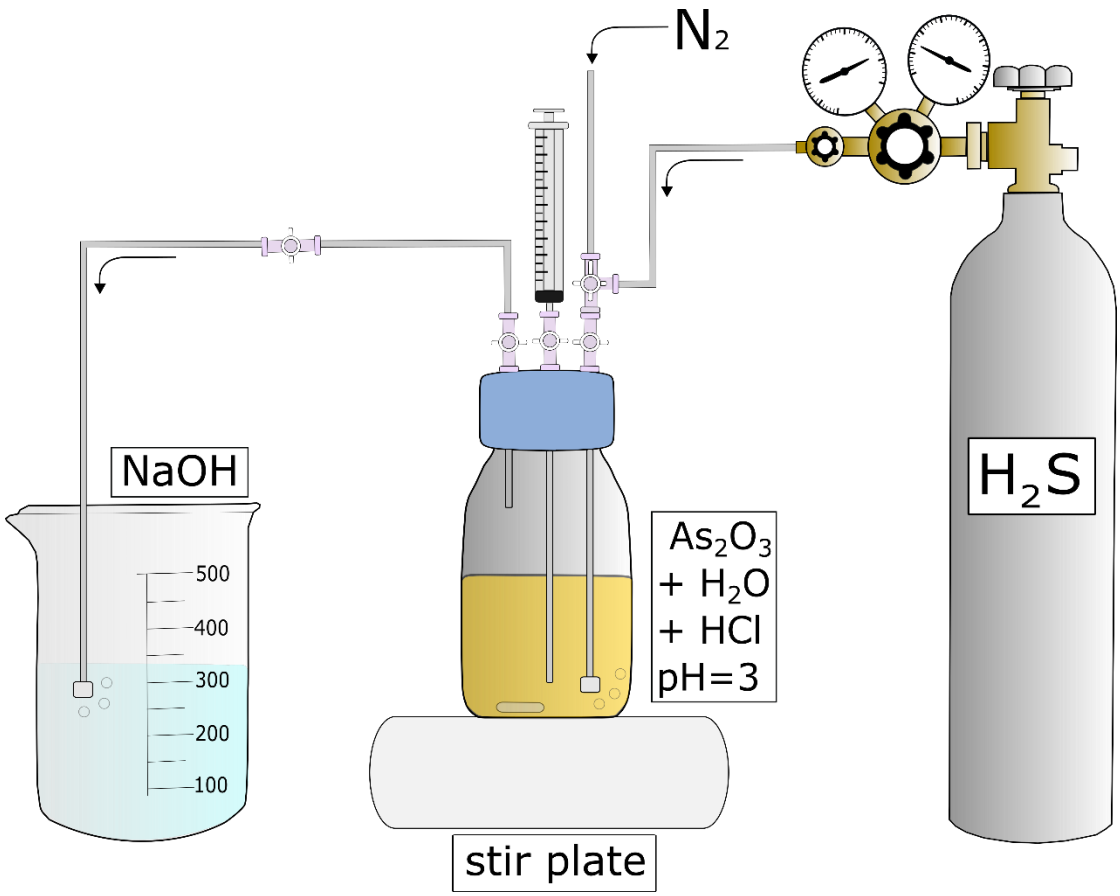

Figure 2-3: Experimental setup for heterogeneous sulfidation of reagent-grade As_2O_3.

The alkalinity, or acid consumption of the Na_2S solution was investigated by simulated acidification of an Na_2S solution using PHREEQC. The simulation involved titration of an aqueous solution containing 0.1 moles of Na_2S with HCl (input file: Appendix B, File 2).

2.3.1. As_2O_3 solubility and dissolution rates above 100 ºC

The As_2O_3 present in the Giant Mine dust must be dissolved in order to create the conditions necessary for a homogeneous sulfidation reaction. This requires knowledge of the solubility and dissolution rate versus temperature to assist in designing a treatment process. The dissolution of the As_2O_3 was initially explored using reagent-grade As_2O_3 in experiments designed to measure the solubility and dissolution rate versus temperature in distilled water (140 °C, 160 °C, 180 °C, 200 °C) using a CEM Discover® SP microwave. Temperature is the primary control variable for the experiments, but the microwave system is designed to

allow pressure of the reaction system to follow the saturation vapour pressure at any given temperature. The microwave functions by heating a sealed vessel to a designated temperature, corresponding vapour pressure, and time, and the reaction time refers to the duration that the vessel remains at the programmed temperature. The ramp-up heating time required to obtain each programmed temperature ranged between 1.5 and 2.5 min, and cooling times ranged between 0.5 and 1.7 min. The ramp-up and cooling times for a sample heated to 200 ^{o}C are displayed in Figure 2-4.

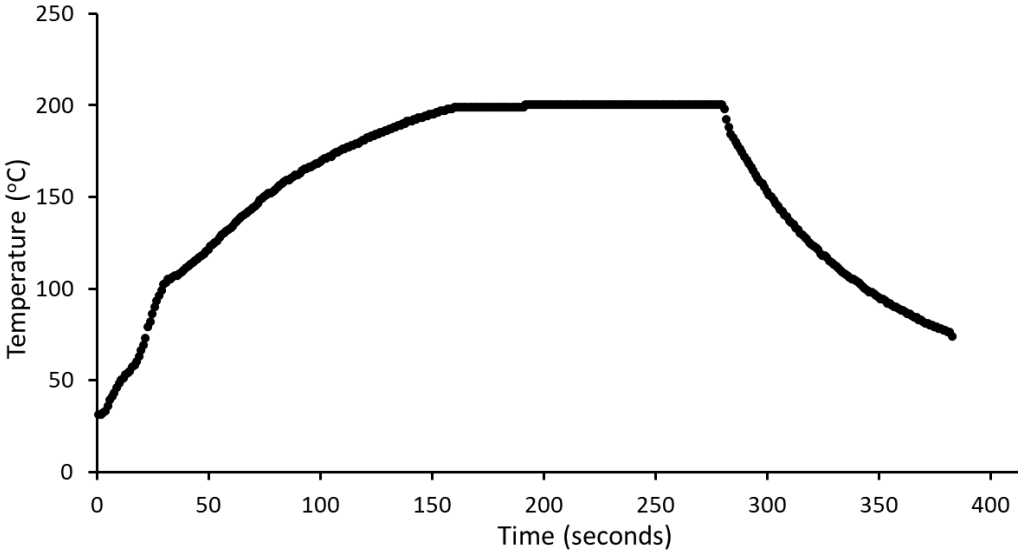

Figure 2-4: Typical ramp-up and cooling times for a sample heated to 200 ^{o}C.

When a mass of As_2O_3 powder is reacted with water in the glass reaction vessel, a video camera allows for visual determination of the time required to achieve complete dissolution. A measure of the dissolution rate is obtained from this time-to-dissolution data when it is acquired at a constant temperature from multiple experiments, each with incremental increases in the mass of As_2O_3. The time-to-dissolution is recorded with each incremental mass and the solubility limit is defined as the concentration of As_2O_3 at which complete dissolution of the As_2O_3 is no longer observed.

There are two principal sources of uncertainty in the solubility and dissolution-rate experiments: a) that from visual estimates of the time to disappearance of As_2O_3 within the reaction vessel, and b) the mass of

As_2O_3 dissolved during the temperature ramp up. An estimate of uncertainty in the visual determinations of the time-to-dissolution is provided by the standard deviation for triplicate measurements at both 140 ^oC and 180 ^oC. There is no satisfactory way to determine the mass dissolved during temperature ramp up versus that dissolved at the target temperature, so the reaction rates are considered apparent rates.

2.3.2. Dissolution of As_2O_3 in Giant Mine material (B233-P9)

Impurities, particularly Sb, are expected to decrease the solubility of As_2O_3 contained in the Giant Mine dust relative to reagent grade As_2O_3 and may also affect the dissolution rate (CANMET, 2000; Section 1.3.4). The Giant Mine dust contains a variety of mineral components, some of which have very low solubility and will therefore remain as a residue after dissolution of the As_2O_3. The ability to dissolve the As_2O_3, the fraction of the initial Giant Mine material that remains as a residue, and the residue composition were all investigated with aqueous extractions. Approximately 250 mg of dust in 4 mL of distilled water were heated to temperatures of 140 °C, 160 °C, 180 °C and 200 °C over durations of 10, 20, and 30 min in a CEM Discover® SP microwave (Figure 2-5). Due to the magnetic properties of the dust, the sample was easily brought into suspension with the instrument's electromagnetic stirring mechanism, so stir bars were not used. After the heating period, each sample was cooled to 70 ^oC, and immediately diluted (4 mL:40 mL) in a 50 mL centrifuge tube. The samples were then centrifuged at 3000 RPM for 12 minutes, the supernatant was decanted, and the solid residues were dried in air.

This approach results in uncertainty in the mass of As_2O_3 extracted because some reprecipitation may occur during cooling of the vessel to a point at which the vial can be safely opened (70 to 100 ^oC; Figure 2-4). To quantify the extent of As_2O_3 reprecipitation upon cooling, a known mass of As_2O_3 and water was dissolved at 140 ^oC, 160 ^oC, 180 ^oC, and 200 ^oC. The samples were cooled to 100 ^oC, poured into a syringe, and filtered (0.2 µm nylon syringe filter). The solution was diluted with 1% HCl and the total dissolved As concentration was determined by ICP-OES and compared to the known initial mass of As_2O_3.

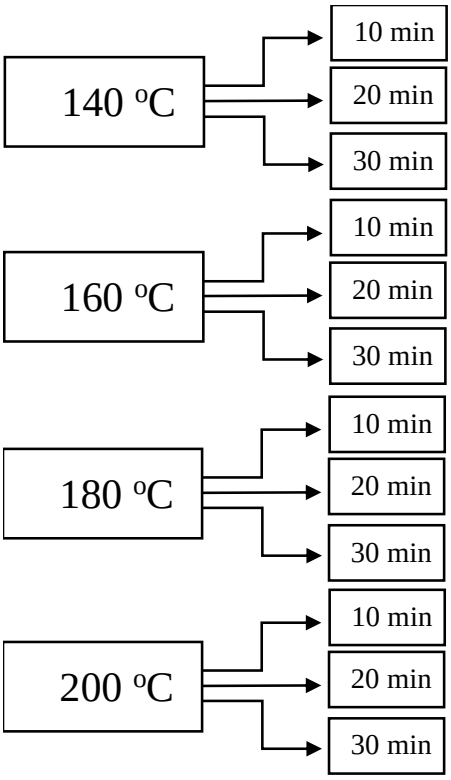

Figure 2-5: Sample B233-P9 extraction temperature and time conditions.

2.4. Characterization of reaction products and residues

2.4.1. Heterogeneous sulfidation reaction products

The dried yellow powder obtained after reaction of H_2S (g) with a slurry containing reagent-grade As_2O_3 in water (pH=3) was characterized with X-Ray Diffraction (XRD) using a Rigaku Ultima IV diffractometer equipped with a Cu source; scanning from 10 º to 40 º (2θ) at a scan rate of 1 º per minute. Phase identification was done using ICDD's PDF-2 software. The powder was further analyzed by Elemental Analysis (EA) using an Elementar VarioEL Cube EA to quantify sulfur. Finally, the sample was mounted in epoxy, polished in kerosene to reveal cross sections of the powder grains, and analyzed with Scanning Electron Microscopy and Energy Dispersive Spectroscopy (SEM-EDS). Back-scattered electron (BSE) images and EDS analyses were acquired using a JEOL 6610LV SEM (accelerating voltage of 20 kV) with an Oxford INCA large area SDD detector.

2.4.2. Extraction residue from the Giant Mine sample B233-P9

The dried B233-P9 extraction residues were weighed to determine the fractional mass retained in each residue after the extractions. To allow for calculation of the elemental fractions retained in the residues, ≈3 mg of each residue was digested in 1 mL of concentrated aqua regia and analyzed by ICP-OES as described in Section 2.1. The elemental fractions retained were determined as:

$$\%\ elemental\ fraction\ retained = \frac{Mass\ of\ element\ in\ residue}{Mass\ of\ element\ in\ initial\ sample} \times 100\% \quad [6]$$

In order to determine the forms of As remaining in the residue and attempt to identify the residual mineral phases, a fraction of the residual solids was embedded in epoxy and prepared for SEM-EDS imaging and analysis as described in Section 2.1.

3. Results

3.1. Material characterization

3.1.1. Reagent-grade As_2O_3 characterization

The reagent-grade arsenic trioxide powder was pure white in colour. Back Scattered Electron (BSE) imaging of the reagent-grade As_2O_3 revealed euhedral grains ranging in grain size from approximately 5 to 50 µm (Figure 3-1).

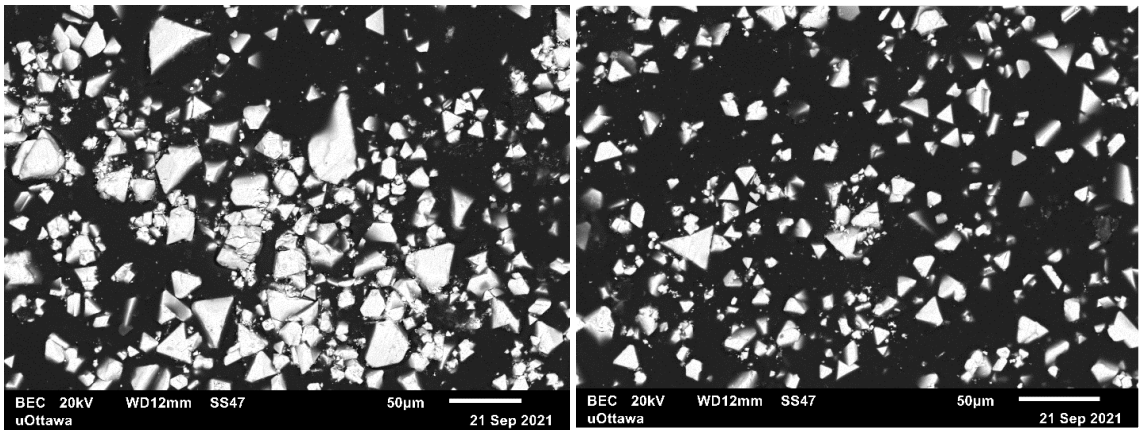

Figure 3-1: BSE images of reagent-grade As_2O_3.

3.1.2. Giant Mine sample B233-P9 characterization

The Giant Mine B233-P9 material has previously been geochemically and mineralogically characterized (CANMET, 2000; SRK, 2004). A subsample was used throughout this research; this subsample was analysed geochemically to determine its initial concentrations to be used in the extraction experiments outlined in Section 2.4.2.

Although the coarse fraction yielded lower average arsenic and higher average antimony concentrations than the finer fraction (Table 3-1), their respective error bounds overlapped. The complete dataset is listed in Appendix A, Table 2.

The geochemical data are in good agreement with the previous geochemical analyses (SGS Lakefield, 2004; Figure 3-2), confirming that sample B233-P9 contains high Sb and Fe, and low As concentrations relative to most other Giant Mine samples.

3.2. Heterogeneous As_2O_3 sulfidation

3.2.1. Modelling

Results of geochemical modeling indicate that the reaction between H_2S and solid As_2O_3 is thermodynamically favourable, resulting in a linear decrease in As_2O_3 and corresponding increase in As_2S_3 (Figure 3-3). The pH is invariant until As_2O_3 is fully consumed, after which it decreases from 6 to ≈3.5 due to the presence of excess H_2S.

Table 3-1: Elemental concentrations determined from coarse aggregates and fine material in sample B233-P9.

Element	Coarse Aggregates		Fine Material		Fine + Coarse Material	
	Mean Concentration *mg/kg (n=10)*	RSD (%)	Mean Concentration *mg/kg (n=5)*	RSD (%)	Mean Concentration *mg/kg*	RSD (%)
As	4.038×10^5	7.370	4.442×10^5	4.393	4.172×10^5	7.878
Sb	1.443×10^4	9.808	1.307×10^4	2.724	1.398×10^4	9.610
S	N/A	N/A	1.069×10^4	4.746	1.069×10^4	4.746
Fe	9.016×10^4	5.787	9.253×10^4	3.232	9.095×10^4	5.201
Al	6507	5.992	6143	3.216	6386	5.937
Ca	9442	8.309	6700	2.589	8528	16.96
Mg	5466	6.160	4430	2.037	5121	10.99
K	1151	6.630	187.7	3.228	830.2	55.24
Zn	1658	4.908	1617	4.746	1644	4.999
Na	596.7	11.06	218.1	8.005	470.5	39.68
Pb	3946	6.014	4108	2.670	4000	5.441
Cu	640.9	6.043	501	3.361	594.3	5.201

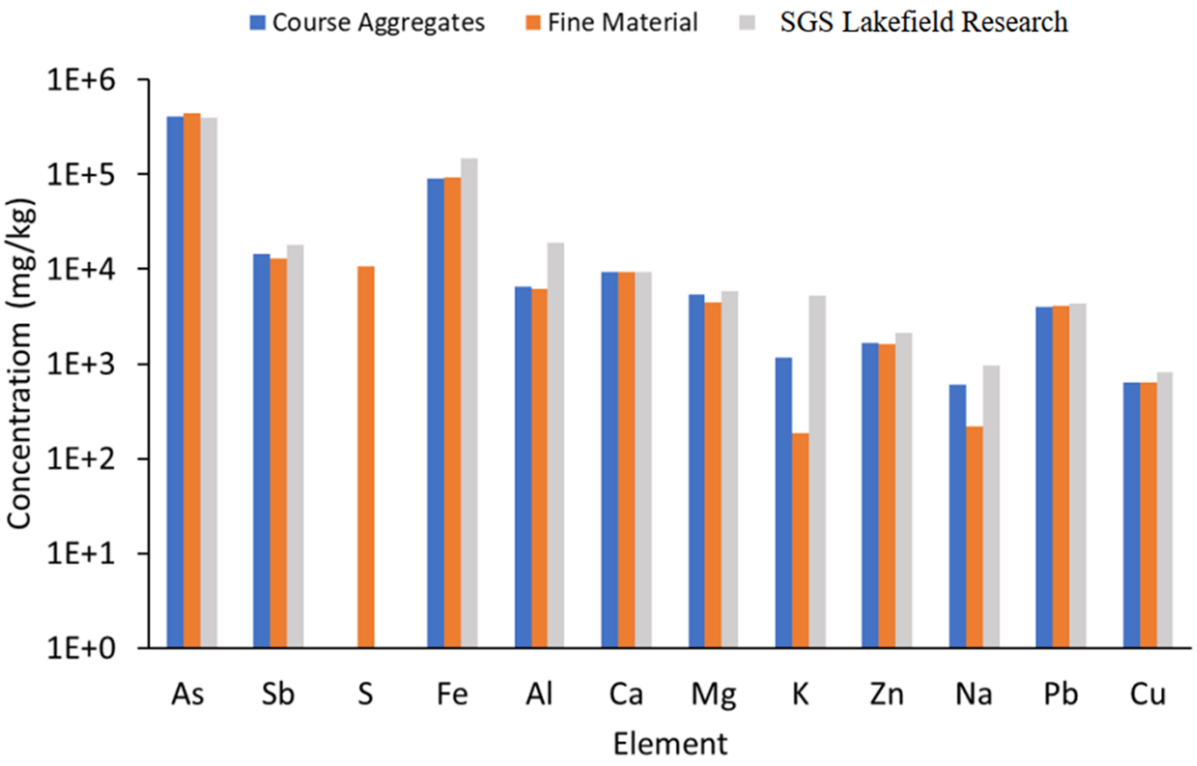

Figure 3-2: Comparative elemental concentrations, on a logarithmic scale, between coarse and fine material (mean), and a previous laboratory analysis (SGS Lakefield Research, 2004) for sample B233-P9.

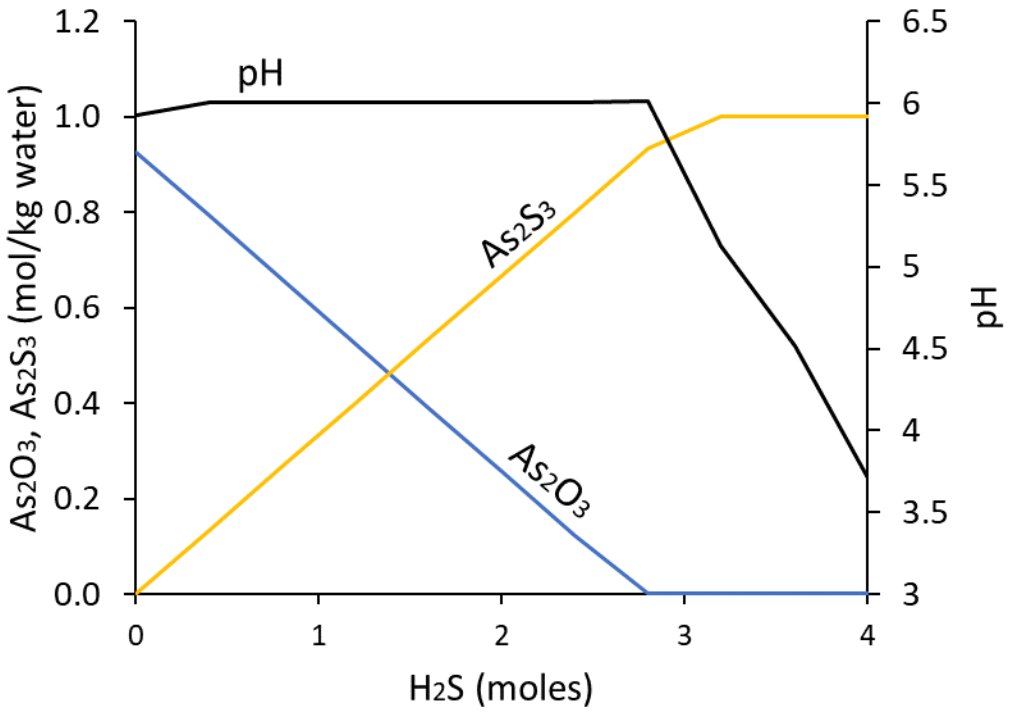

Figure 3-3: Results of PHREEQC modelling showing linear increase in As_2S_3 and decrease in As_2O_3, corresponding to addition of H_2S.

3.2.2. Experimental

While injecting $H_2S_{(g)}$ in an acidified As_2O_3 slurry, the white As_2O_3 powder turned bright yellow within the first 5 minutes of the experiment (Figure 3-4). The slurry remained yellow and opaque for the remainder of the experiment (Figure 3-5).

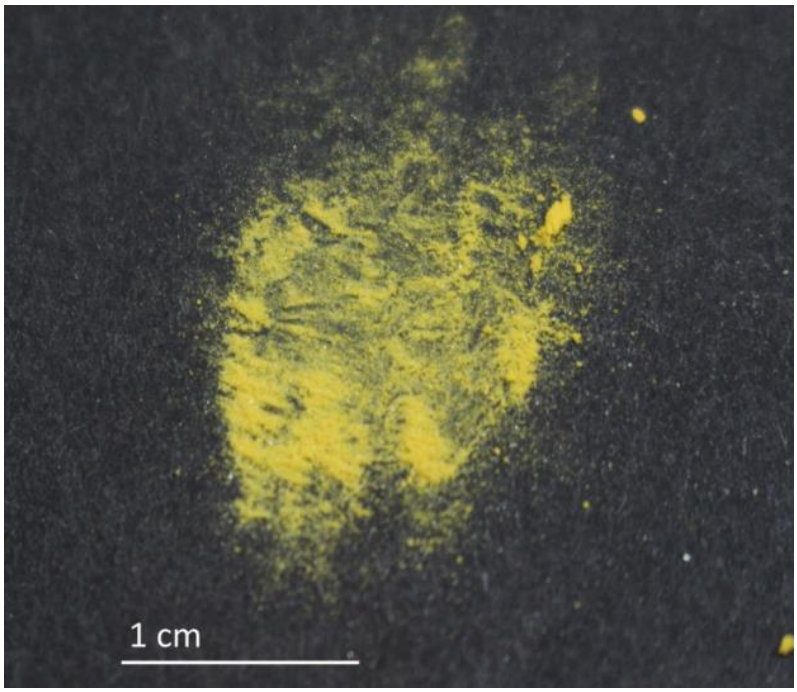

Figure 3-4: Product from reaction of an As_2O_3 slurry with H_2S $_{(g)}$.

Figure 3-5: Aqueous slurry of As_2O_3 reacted with H_2S $_{(g)}$.

After collecting and drying the yellow precipitate (Figure 3-4), XRD results revealed the presence of As_2O_3; no crystalline form of As_2S_3 (orpiment), or any other As-S phase, was detected (Figure 3-6). Minor peaks

observed at 22.7 and 26.7 degrees are unidentified, but a database search in the XRD phase identification software found no indication that they relate to any known As- S- O-bearing phase.

Analysis of the powder with EA indicated that the reaction product contains 1.09 wt.% S, whereas pure As_2S_3 should contain 39 wt.% S. Analysis of the reaction product by SEM-EDS (Figure 3-7) indicates that these grains are composed primarily of As and O, although a trace of sulfur was detected on the edge of a single grain.

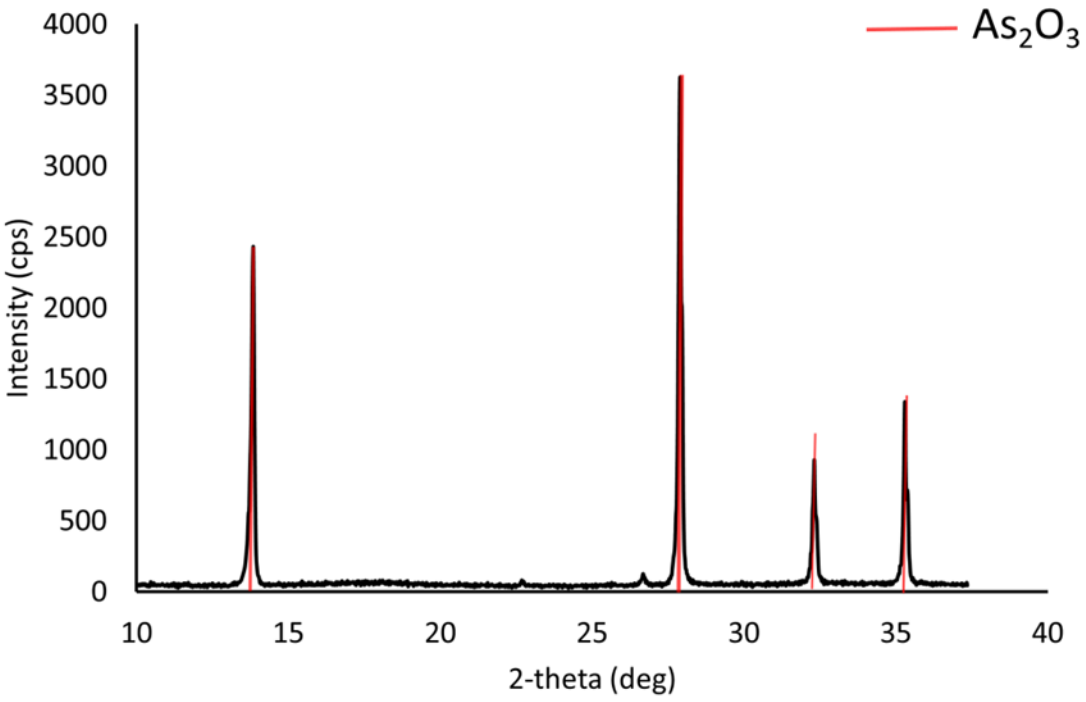

Figure 3-6: XRD pattern for the product of a heterogeneous reaction between As_2O_3 and $H_2S_{(g)}$.

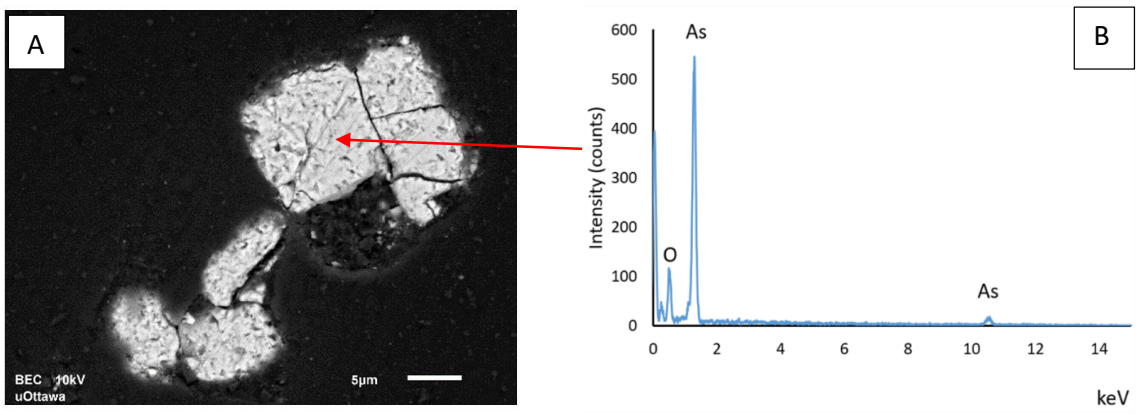

Figure 3-7: BSE image (A) and EDS spectrum (B) for the product of a heterogeneous reaction between As_2O_3 and H_2S.

3.3. Homogeneous As_2O_3 sulfidation

When the As (III)- and S^{2-}-containing solution was titrated with 1.6 N H_2SO_4 (Section 2.3), a fine yellow precipitate formed at the tip of the titrator as the H_2SO_4 was added. The initial pH was 13.07, and as it decreased toward the final pH of 7.73, the yellow precipitate formed a dense, opaque slurry (Figure 3-8). The formation of the As_2S_3 precipitate was nearly instantaneous upon addition of acid, demonstrating a very rapid reaction rate for the homogenous sulfidation reaction. The titration from pH 13.07 to 7.73 required 13 mL of 1.6 N H_2SO_4.

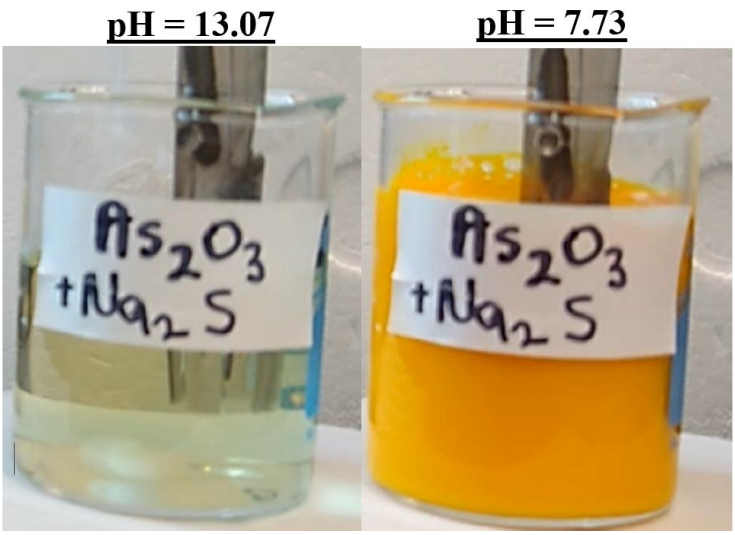

Figure 3-8: Solution containing dissolved As_2O_3 and $Na_2S \cdot 9H_2O$ (left), and the As_2S_3 precipitate formed by acidification (right).

The model (PHREEQC) titration of a 1-L solution containing 0.1 moles of Na_2S indicates that 0.195 moles of HCl are required to lower the pH from an initial value of 13 to 5.5, as indicated in **Error! Reference s ource not found.**.

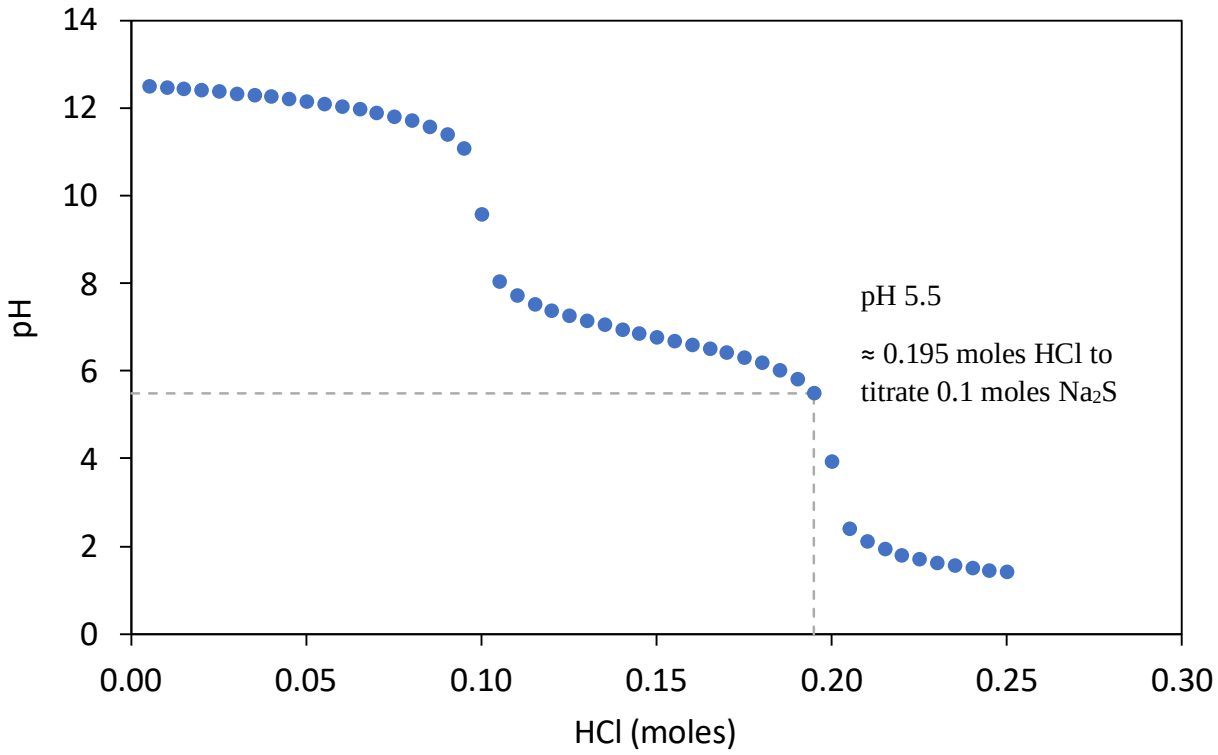

Figure 3-9: Results of PHREEQC modelling showing titration of solution containing dissolved Na_2S with HCl.

3.3.1. As_2O_3 solubility and dissolution rates above 100 °C

A homogenous sulfidation reaction for treating the Giant Mine dust requires an initial dissolution step. The time-to-dissolution for various concentrations of As_2O_3 at 140 °C and 180 °C are displayed in Table 3-2 and Figure 3-10. The results inform the dissolution rate for reagent grade As_2O_3 at each temperature.

The initial dissolution rate of As_2O_3 was rapid at both temperatures; at 140 °C, 89 % of the As_2O_3 dissolved in five minutes, and at 180 °C, 93.7 % of As_2O_3 dissolved within four minutes of heating (Table 3.2). The times-to-dissolution are displayed in Figure 3-10, along with data at 60 °C for comparison (CANMET,

2000). Error bars for the time determination were constructed by conducting triplicate dissolution experiments at 140 °C and 180 °C. The error bars represent the relative standard deviation between these triplicate values for Figures 3-10, 3-11.and 3-12.

Table 3-2: Time-to-dissolution for As_2O_3 at 140 °C and 180 °C

140 °C		180 °C	
Final Concentration (g As_2O_3/kg water)	Time (min)	Final Concentration (g As_2O_3/kg water)	Time (min)
165.2	5	185.8	2
169.2	7	205.9	2.5
175.0	10	212.7	3
176.4	12	235.1	4
180.1	20	240.2	10
183.9	25	245.7	18.5
185.7	33	250.6	60

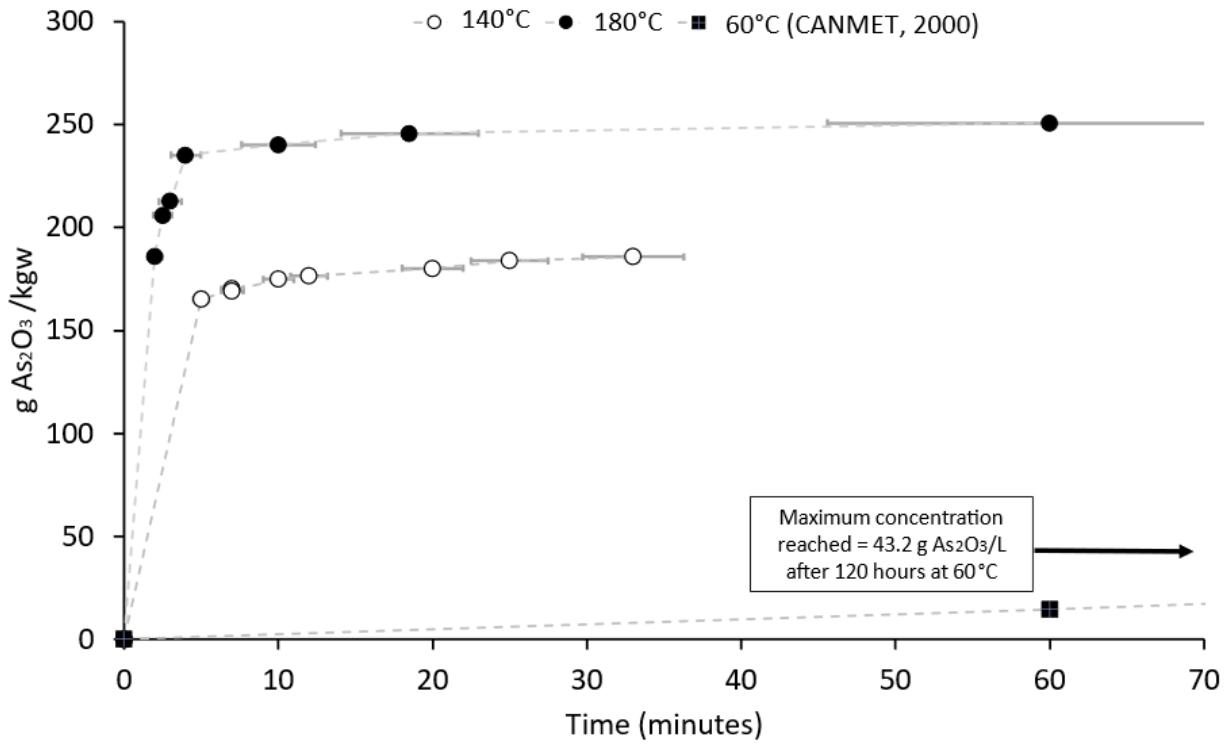

Figure 3-10: Time-to-dissolution for As_2O_3. The data for 140 °C and 180 °C are from the present study; data for 60 °C are from CANMET (2000).

The highest concentration, or 'upper limit', of As_2O_3 to dissolve at 140 °C and 180 °C, was designated as the concentration at which the solution reached equilibrium with As_2O_3. These concentrations were therefore determined to be the As_2O_3 solubilities at each temperature. At 140 °C, the As_2O_3 dissolved completely when the concentration was 185.7 g As_2O_3/kg water, but when the concentration was increased to 186.7 g As_2O_3/kg water, dissolution was incomplete for a monitoring period of 60 minutes (Figure 3-11). As a result, 185.7 g As_2O_3/kg water was designated as the solubility limit at 140 °C. The corresponding solubility limit at 180 °C was 250.6 g As_2O_3/kg water (Figure 3-12).

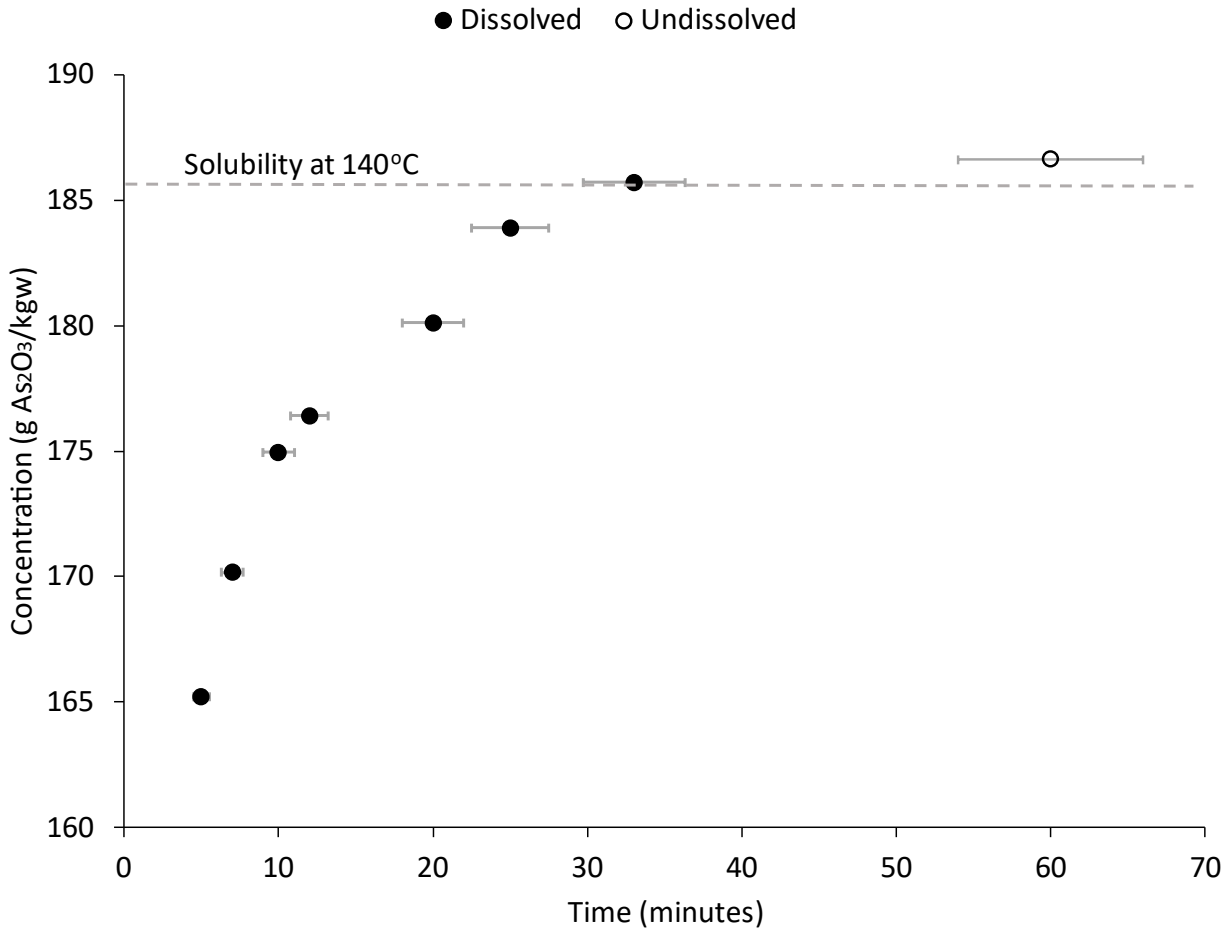

Figure 3-11: Data contributing to the determination of As_2O_3 solubility at 140 °C. Solid circles represent concentrations of As_2O_3 powder that completely dissolved upon heating. Open circles indicate concentrations that resulted in incomplete dissolution.

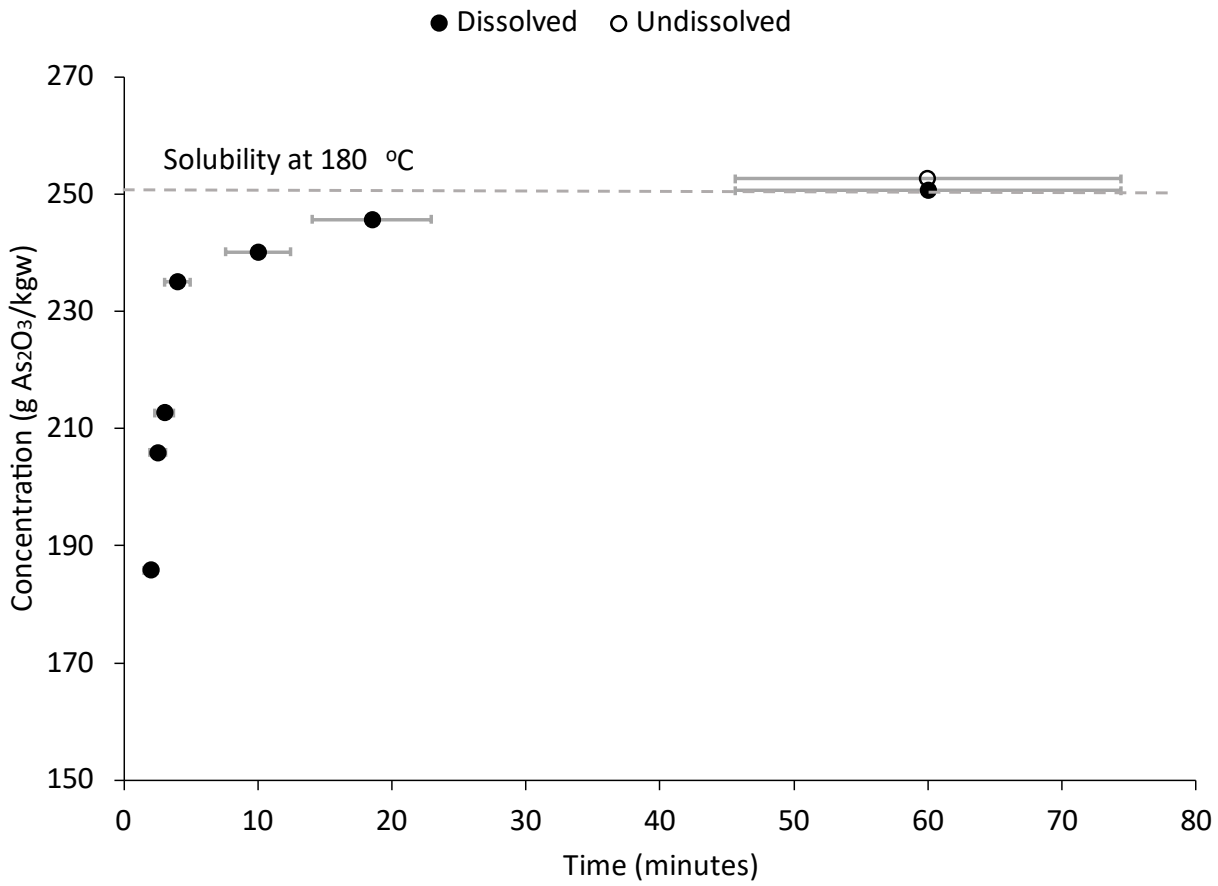

Figure 3-12: Data contributing to the determination of As_2O_3 solubility at 180 °C. Solid circles represent concentrations of As_2O_3 powder that completely dissolved upon heating. Open circles indicate concentrations that resulted in incomplete dissolution.

The As_2O_3 time-to-dissolution data were used to calculate the dissolution rate for As_2O_3 at each temperature as per the equation:

$$\text{rate} = \frac{dC}{dt} \qquad [7]$$

where C is concentration in g As_2O_3/kg water and *t* is time, in minutes. The changes in apparent reaction rate with time at 60 °C (CANMET, 2000), 140 °C, and 180 °C are displayed in Figure 3-13. In each case, the rate decreased with time as was expected because the reaction was approaching equilibrium. The slope of the rate versus time relationship became increasingly negative at higher temperature (Figure 3-14), which was also expected because the approach to equilibrium was more rapid at higher temperature.

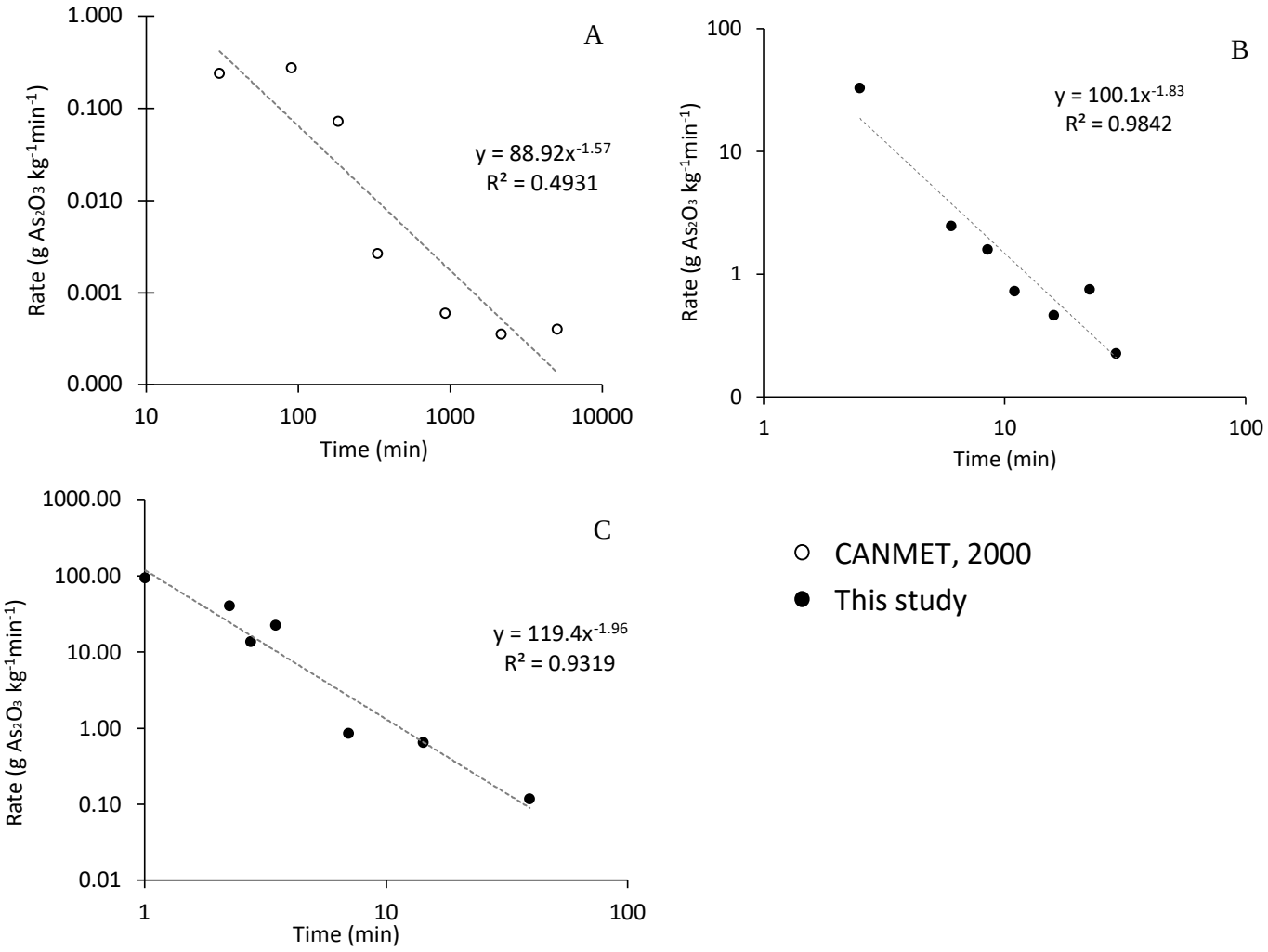

Figure 3-13: Measured As_2O_3 dissolution rates versus reaction time at A) 60 ^oC (data from CANMET, 2000), B) 140 ^oC, and C) 180 ^oC.

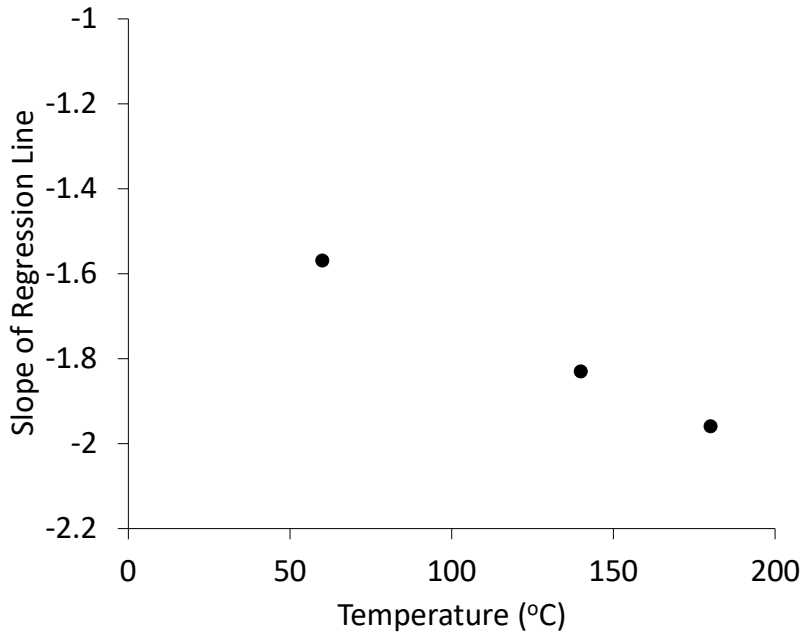

Figure 3-14: Slope of As_2O_3 dissolution reaction rate versus temperature, where the measurement at 60 °C were obtained from CANMET (2000).

While observing the experiments with the camera installed in the CEM Discover® SP microwave, As_2O_3 precipitation was observed during the cooling stage, beginning at approximately 110 °C. Precipitation of As_2O_3 upon cooling was investigated at target temperatures of 140, 160, 180, and 200 °C. Results indicate that the mass of As_2O_3 precipitate removed with the 0.2 μm filter ranged from 11.64% to 15.37% (

Table **3-3**). The mass of precipitate lost from the aqueous system increases systematically with increasing temperature (Figure 3-15).

Table 3-3: Mass of As_2O_3 precipitate (> 0.2 um) formed during cooling to 100 °C

Temperature (°C)	As_2O_3 Concentration (g/kg)		% Mass of As_2O_3 Lost
	Initial Concentration	Measured (ICP-OES)	
140	142.8	125.1	12.4
160	176.9	152.3	13.87
160	144.3	127.5	11.64
160	166.7	143.6	13.87
180	176.1	149.4	15.17
200	181.0	153.2	15.37

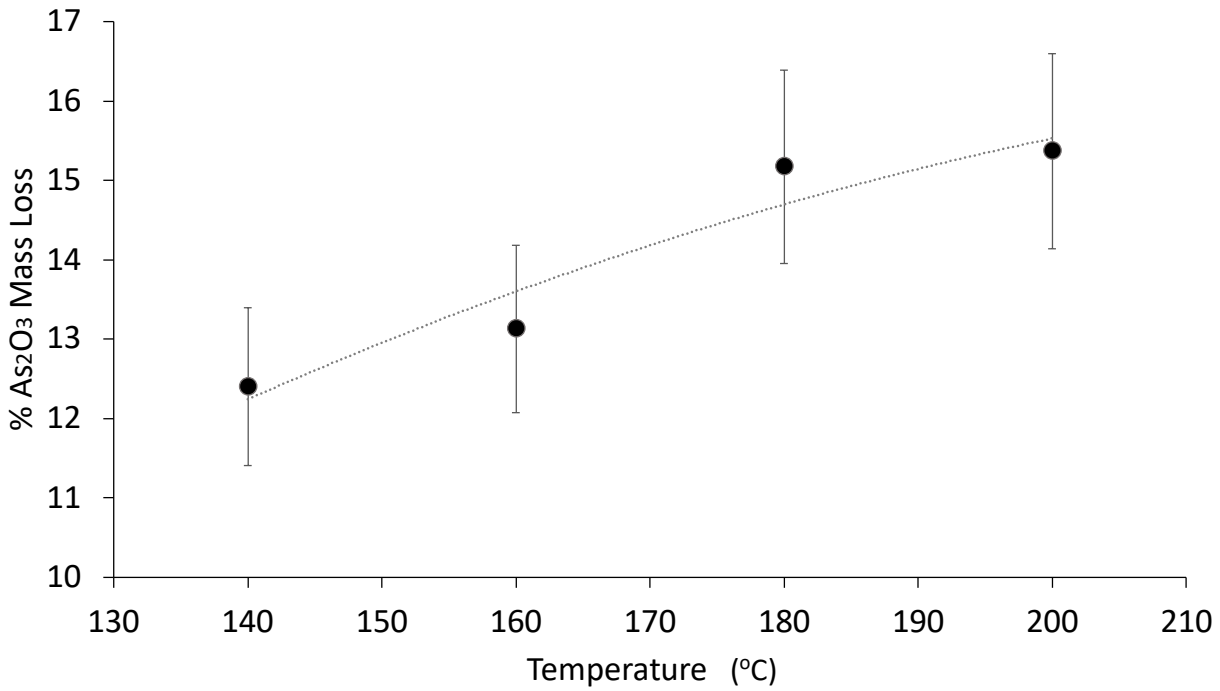

Figure 3-15: Percent of As_2O_3 lost from solution due to precipitation upon cooling. The error bars represent the relative standard deviation for triplicate experiments conducted at 160 °C.

3.3.2 Dissolution of Giant Mine sample B233-P9

Heating the Giant Mine sample B233-P9 at various temperatures and times revealed that an average of 41.74 ± 1.476 wt.% of the sample remained undissolved (Table 3-4). With the exception of the measurements conducted at 140°, there is a slight decrease in residual mass fraction with increasing time, at each temperature (Figure 3-16).

Table 3-4: Residual mass fraction (Giant Mine B233-P9) after extraction experiments

Temperature (°C)	Time (minutes)	Residual Mass Fraction (wt. %)
140	10	41.05
140	20	40.8
140	30	45.25
160	10	42.56
160	20	42.15
160	30	40.71
180	10	43.35
180	20	40.51
180	30	39.56
200	10	42.68
200	20	41.23
200	30	41.1
		Mean: 41.7 Relative Standard Deviation: 3.53 %

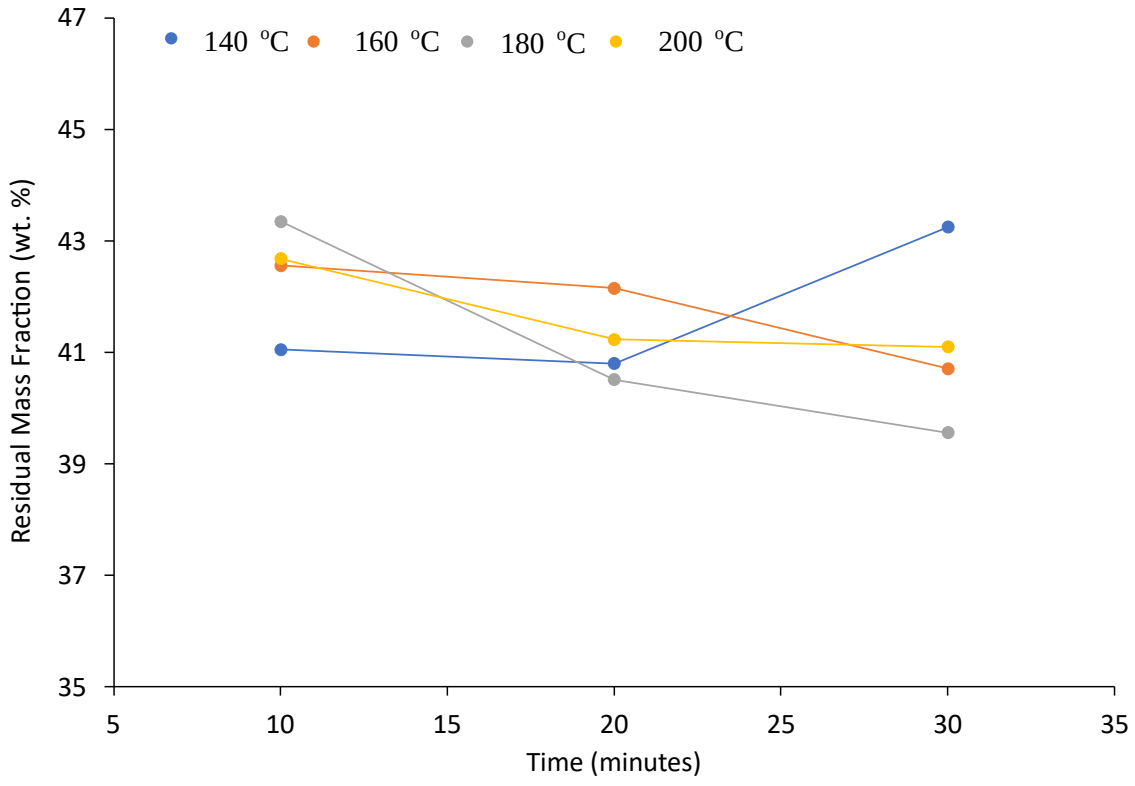

Figure 3-16: Residual mass fraction of dissolved sample B233-P9 versus temperature.

3.3.3 Characterization of Giant Mine sample B233-P9 extraction residue

The fractions of key elements (As, Sb, Fe) that are retained in the residues (Equation 6) from dissolving sample B233-P9 are summarized in Table 3-5; fractions are reported relative to the mean initial concentrations in sample B233-P9 (Table 3-1). The measured mass concentration of all elements is presented in Appendix A, Table 4. The range of respective As, Sb, and Fe remaining fraction percentages across all tested times and temperatures are 18.7 % - 22.52 %, 76.63 % – 83.63 %, and 84.13 – 97.64 %. Figures 3-17, 3-18, and 3-19 display the remaining fraction percentages at each time and temperature, for which the error bars are defined by the remaining fraction percentages calculated relative to the minimum and maximum values from initial concentration replicates (Table 3-1). The percent remaining of As, Sb, and Fe at all times and temperatures fall within the range of the error bars, which represent the heterogeneity within the B233-P9 sample.

Table 3-5: Fractions of critical elements remaining in the Giant Mine residue, relative to mean initial sample concentrations.

Temperature (^{o}C)	Time (min)	% Remaining		
		As	Sb	Fe
140	10	20.19	76.63	87.33
140	20	18.70	78.78	84.13
140	30	22.51	83.63	98.17
160	10	19.85	78.11	94.32
160	20	20.33	77.01	92.53
160	30	19.14	82.11	90.31
180	10	21.45	79.16	98.41
180	20	19.92	79.20	93.66
180	30	20.01	77.28	94.53
200	10	22.52	80.21	97.64
200	20	21.06	78.28	94.94
200	30	21.73	79.51	94.54

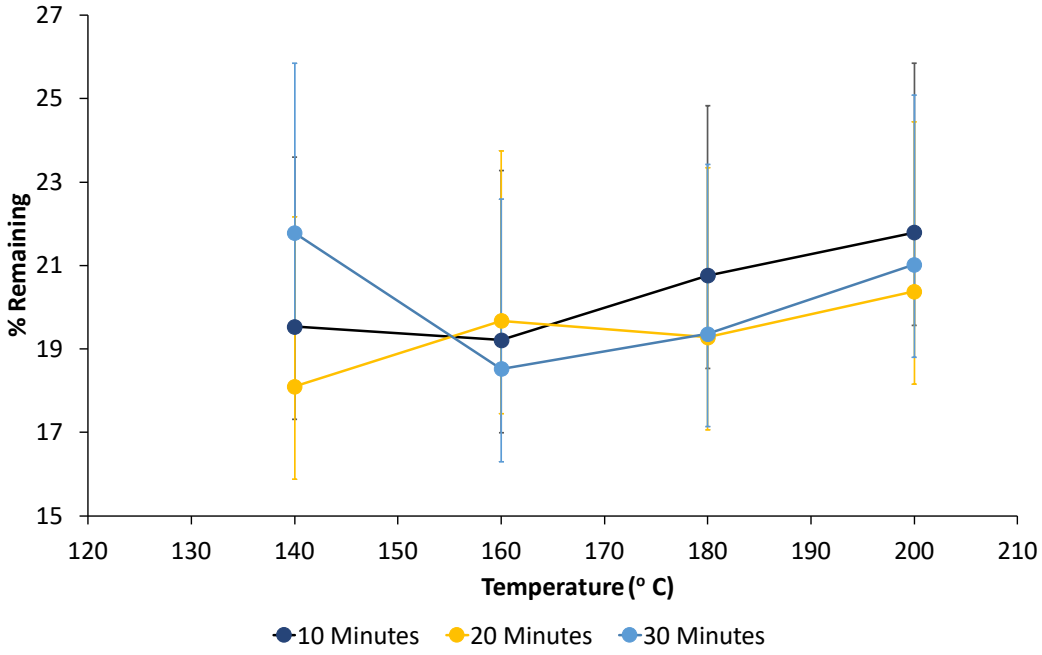

Figure 3-17: Fraction of As remaining in Giant Mine sample B233-P9 residues at various times and temperatures, relative to initial mean sample mass. Error bars represent the fraction of As remaining relative to the range of initial sample masses measured from coarse and fine sample fractions.

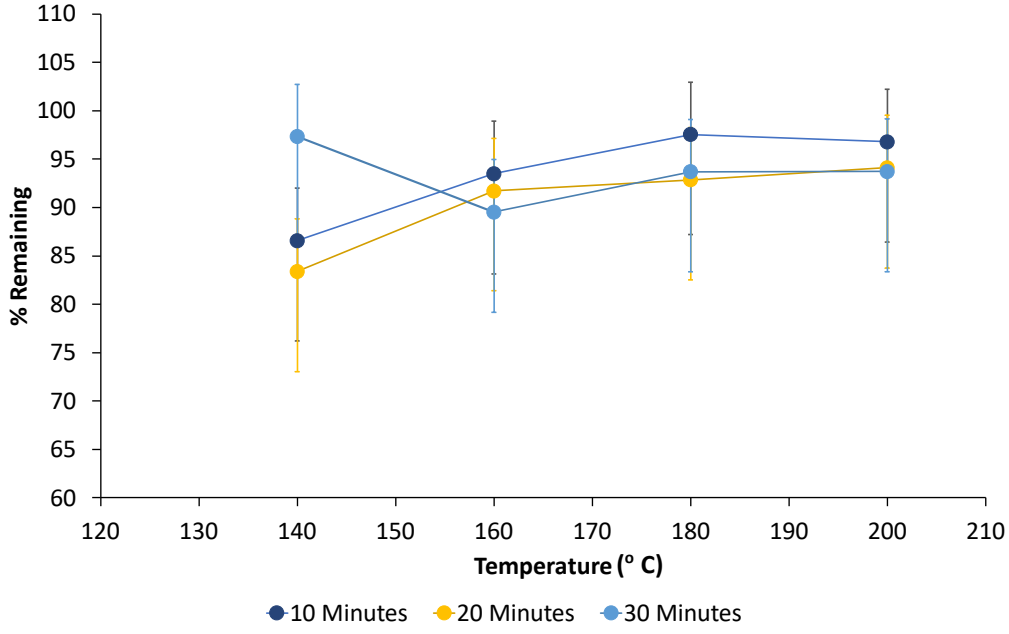

Figure 3-18: Fraction of Fe remaining in Giant Mine sample B233-P9 residues at various times and temperatures, relative to initial mean sample mass. Error bars represent the fraction of Fe remaining relative to the range of initial sample masses measured from coarse and fine sample fractions.

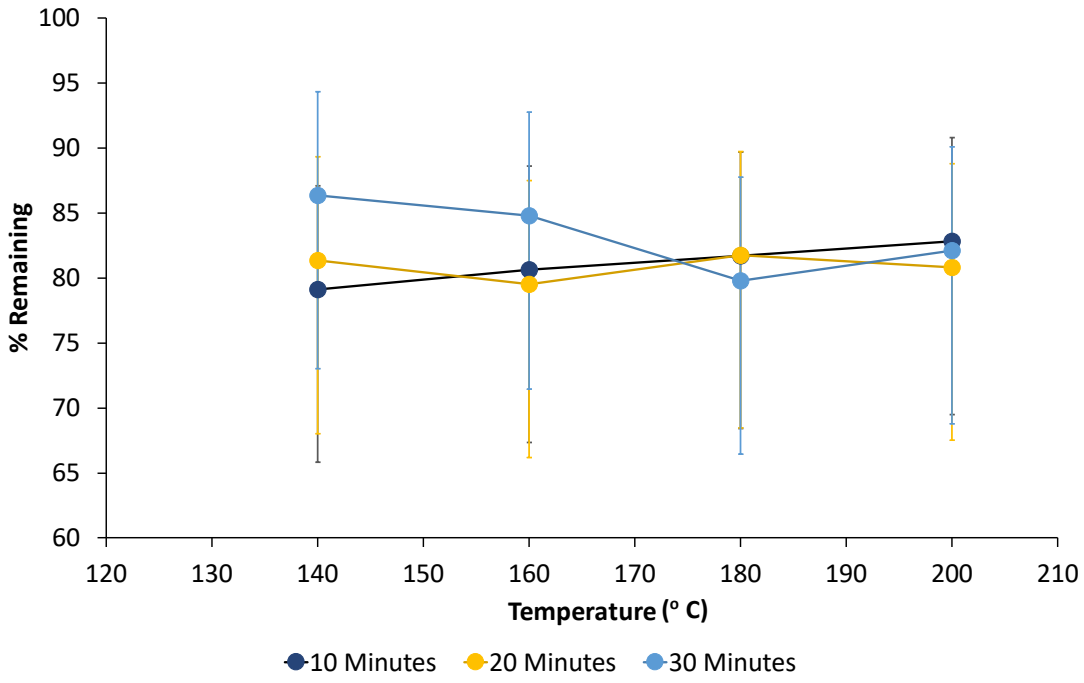

Figure 3-19: Fraction of Sb remaining in Giant Mine sample B233-P9 residues at various times and temperatures, relative to initial mean sample mass. Error bars represent the fraction of Sb remaining relative to the range of initial sample masses measured from coarse and fine sample fractions.

Analysis of the epoxy-embedded residues by SEM-EDS revealed a range of grain sizes; a relatively coarse fraction (1 – 2 mm grains) and a finer fraction (5 – 100 µm grains). A representative BSE image of the fine residue fraction is displayed in Figure 3-20. The principal phases are iron oxides, quartz, and aluminosilicates; however, the majority of residue material is made of up mixed-phase aggregates.

Images and corresponding EDS spectra from point analyses of materials in the fine residue are presented in Figure 3-21 to Figure 3-24. The spectra indicate that most material is As-bearing, particularly Fe-oxides (e.g. Figure 3-21 Spectrum 2), and the mixed-phase aggregates (Figure 3-22 Spectra 1 and 3, and Figure 3-23 Spectra 1 and 2). Additional phases that were observed in the residues, in trace amounts, were native copper, gold, arsenopyrite, Ti-Fe-oxides, and sphalerite.

No As_2O_3 grains were observed in the coarse residue fraction, and minor quantities were observed in the fine residue fraction. Typically, the As_2O_3 grains in the fine fraction were embedded within the mixed

aggregates (Figure 3-20), although a few isolated As_2O_3 grains (up to 3 from each residue subsample) were observed; the largest grain observed is displayed in Figure 3-24 (≈50 µm in length). The EDS analyses indicate that the As_2O_3 grains commonly contain Sb (Figure 3-22, Spectrum 1 and Figure 3-23, Spectrum 2). No As_2O_3 is observed coating or cementing other grains, as would be expected if there was significant As_2O_3 precipitation upon cooling following the high temperature extraction.

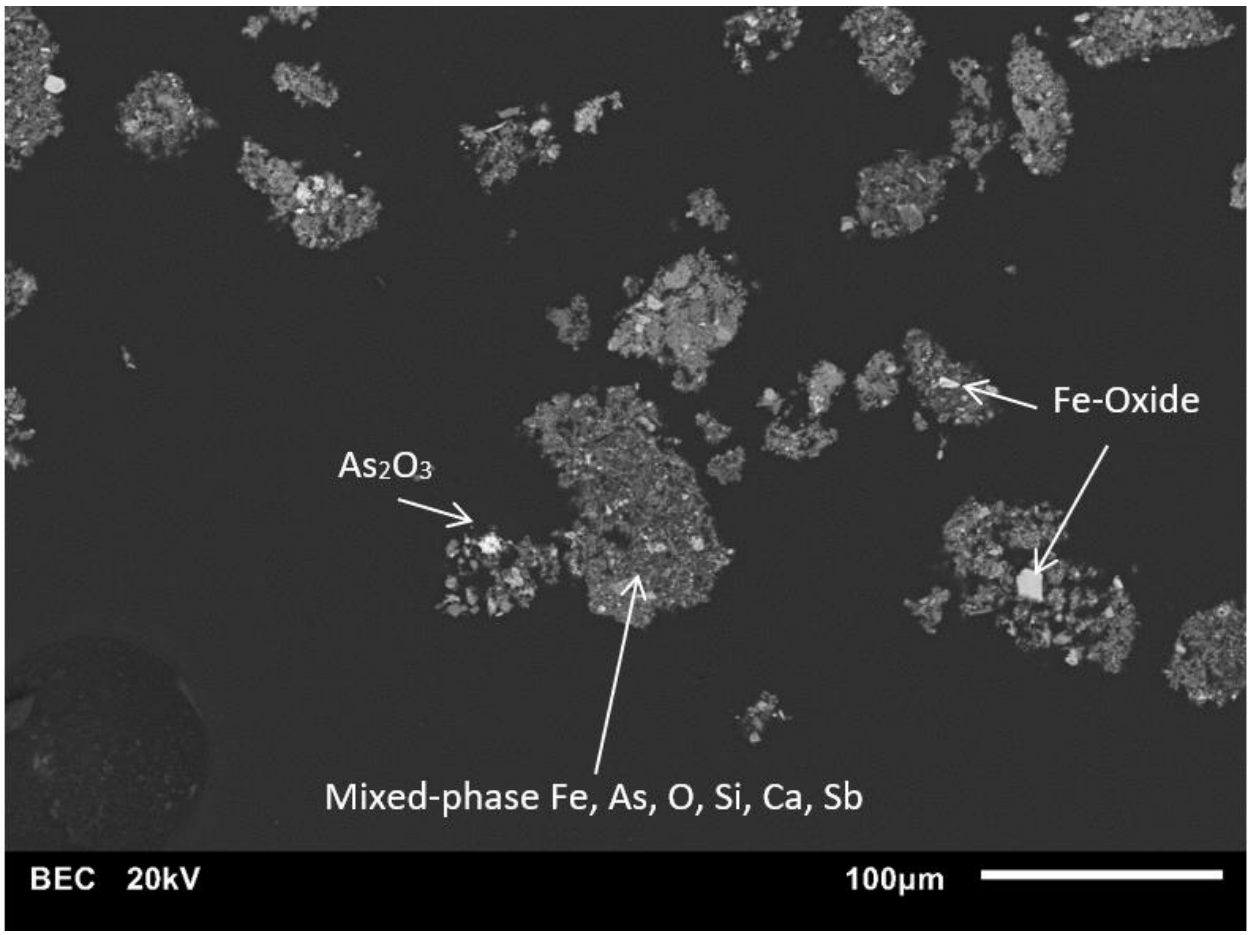

Figure 3-20: Representative backscattered electron (BSE) image of mixed aggregates.

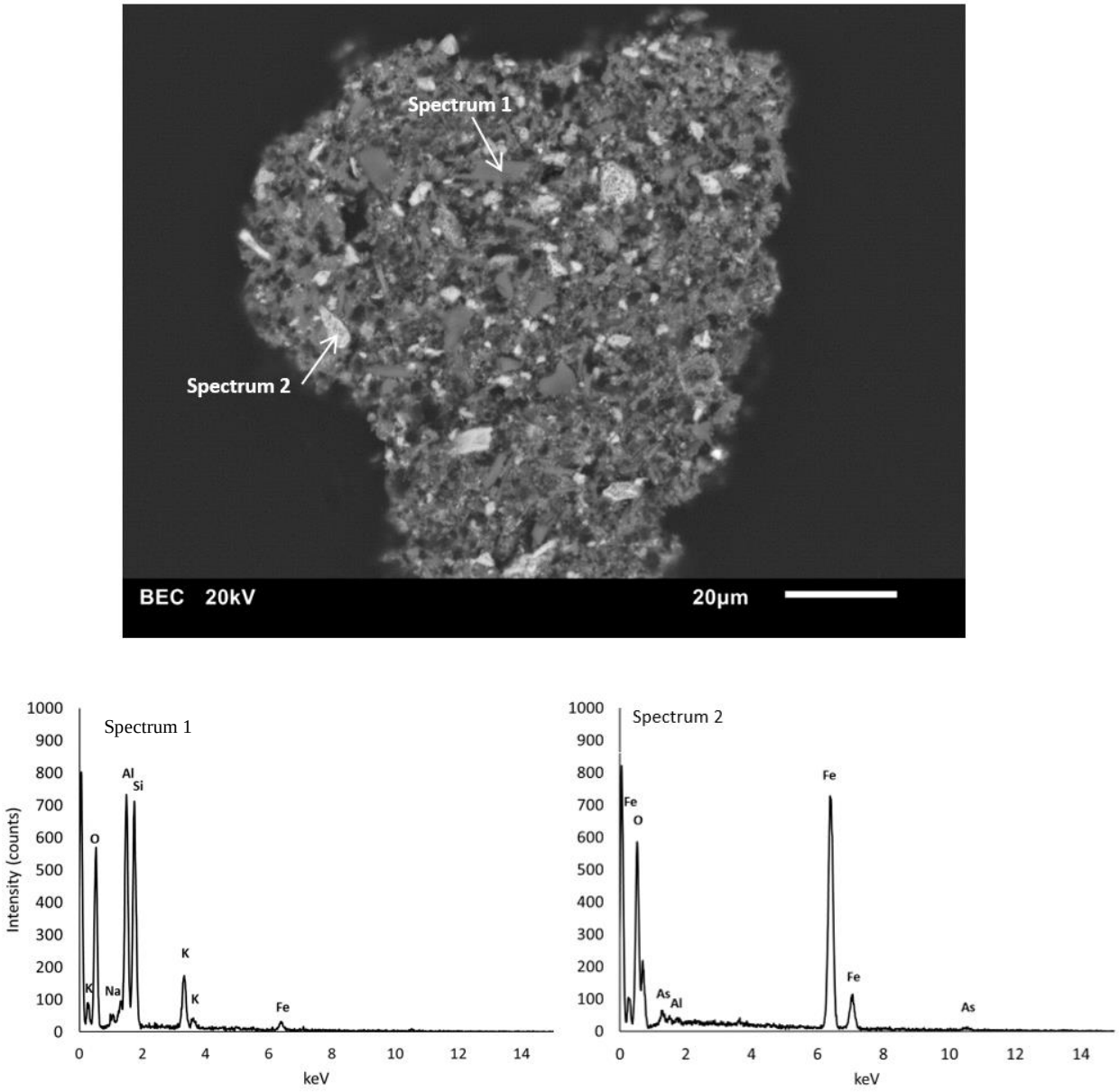

Figure 3-21: SEM BSE image of aggregate containing aluminosilicate phases (Spectrum 1) and Fe-oxide (Spectrum 2) in Giant Mine residue.

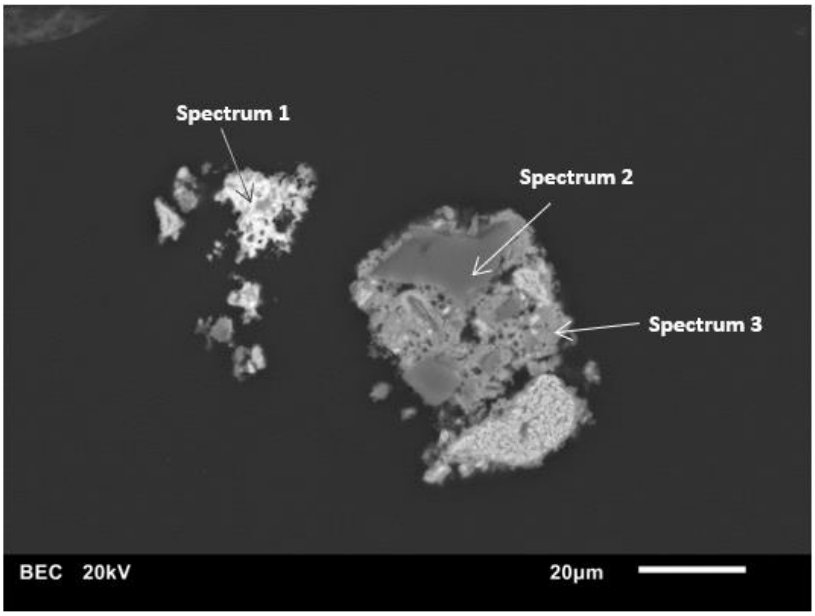

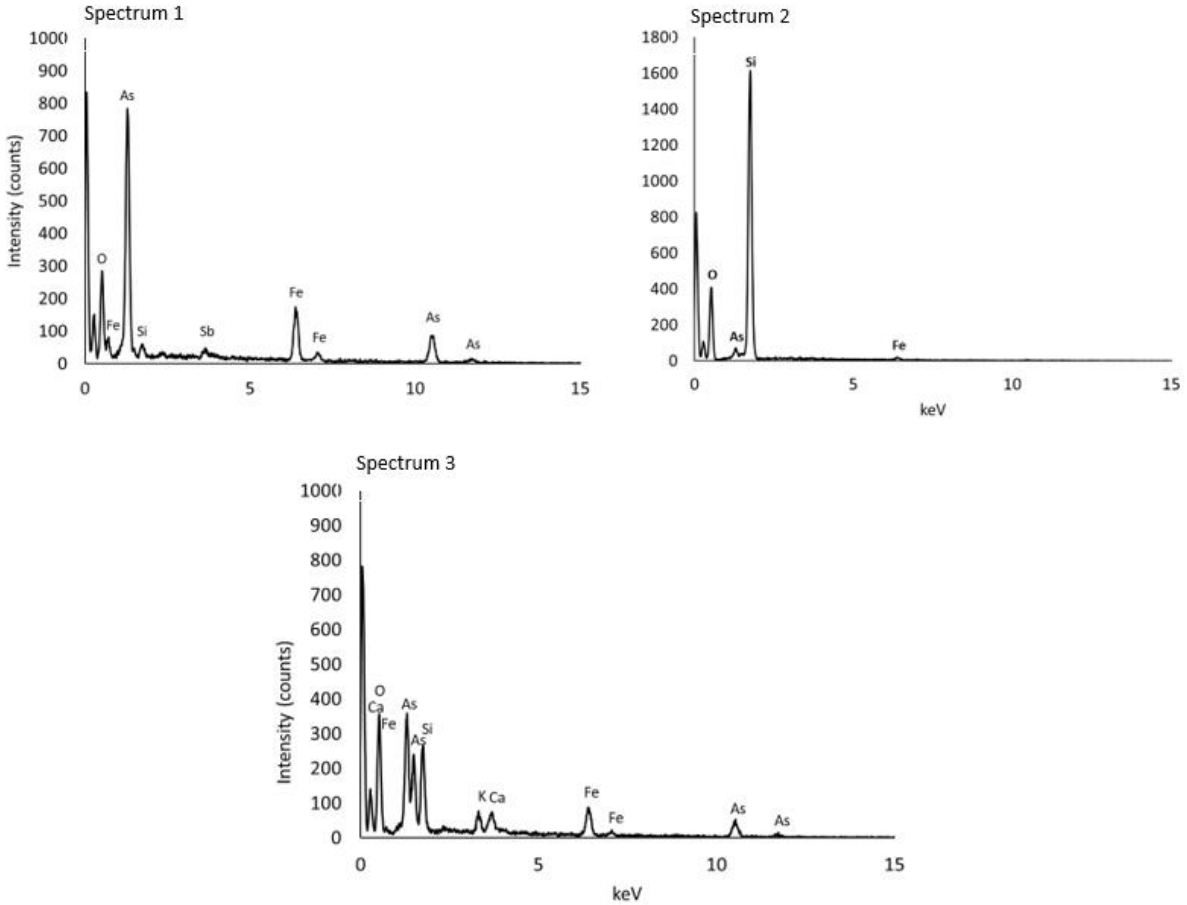

Figure 3-22: SEM BSE image of quartz (Spectrum 2) and other mixed phases, including As_2O_3 (Spectra 1 and 3) in Giant Mine residue.

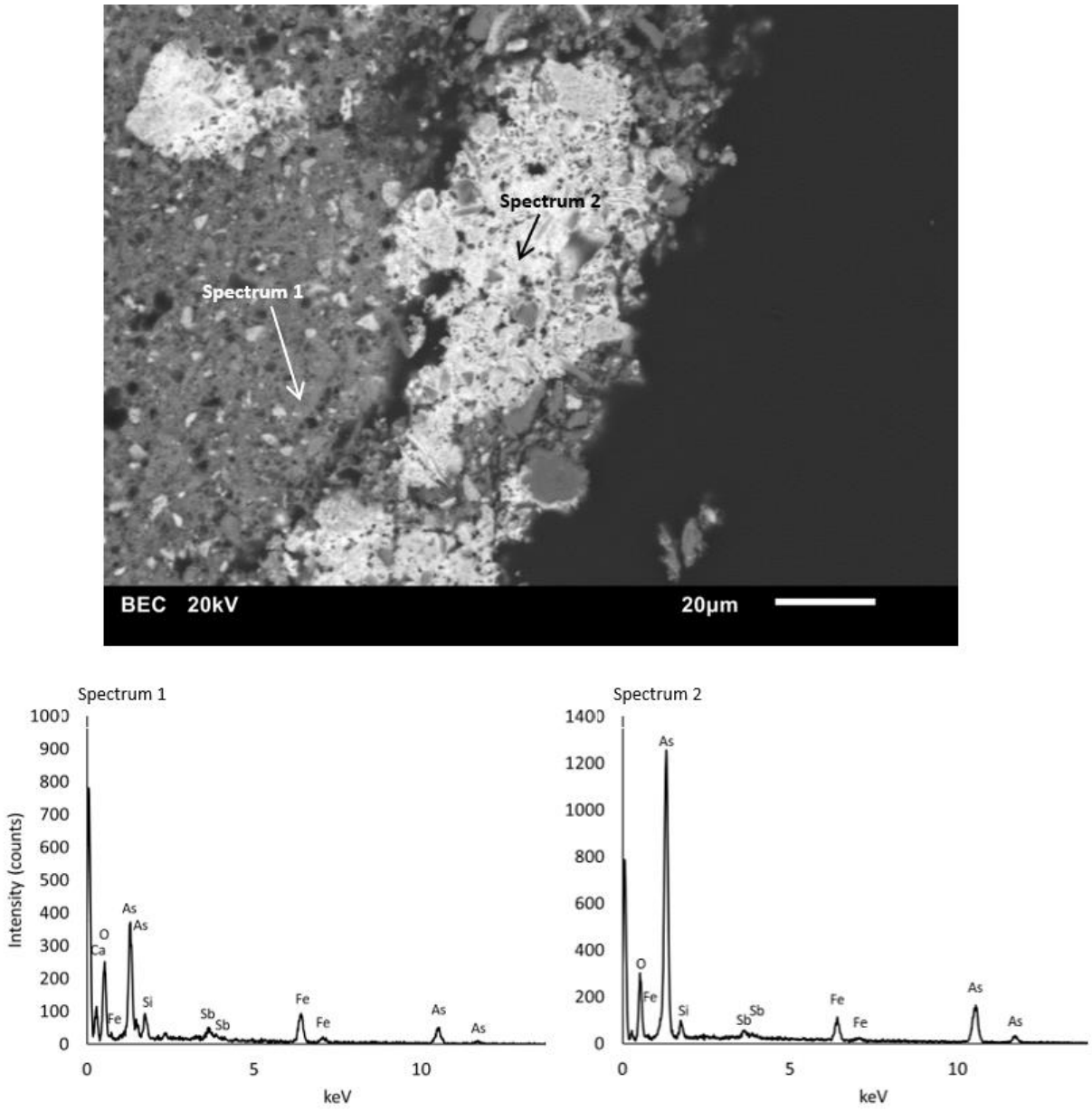

Figure 3-23: SEM BSE image of Sb-bearing phases, where Spectrum 2 is more abundant in As than Spectrum 1.

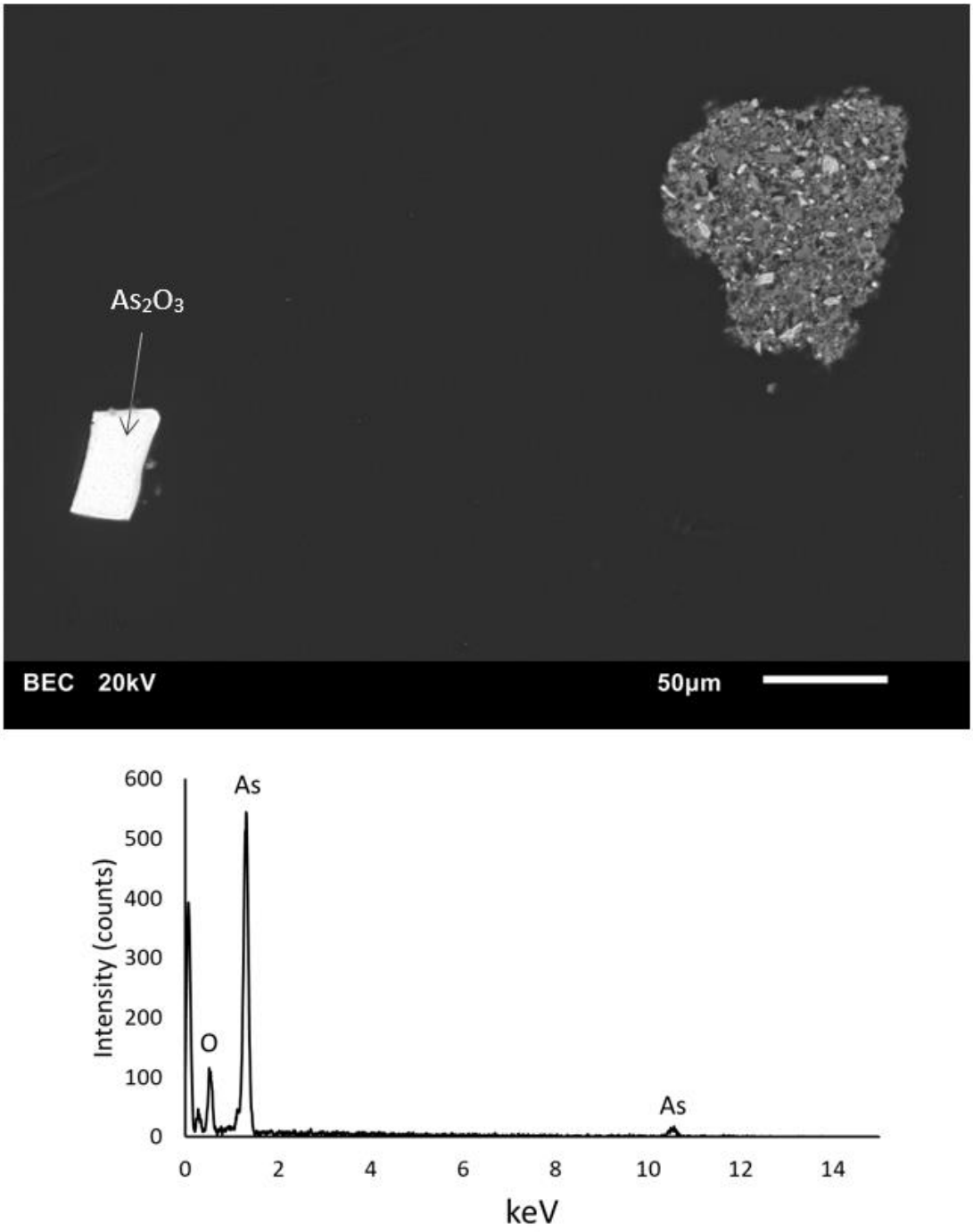

Figure 3-24: SEM BSE image of isolated As_2O_3 grain in Giant Mine residue, with corresponding EDS spectrum of As_2O_3 grain, showing As and O peaks.

4. Discussion

The sulfidation of As_2O_3 has been investigated as a potential long-term remediation strategy for As_2O_3-rich dust at the Giant Mine. While developing methodologies at the laboratory scale, the feasibility of scaling up the procedure to treat 237 000 tonnes of material was a principal consideration in terms of development of the sulfidation technique and the choice of reactants.

4.1. Heterogeneous As_2O_3 sulfidation

Introducing sulfide to a slurry of As_2O_3 was the initial approach investigated to achieve sulfidation. This is a heterogeneous reaction that would not require dissolution of the As_2O_3 prior to sulfidation; a heterogeneous reaction approach could simplify method design and minimize costs associated with large-scale implementation.

Equilibrium geochemical modelling indicates that conversion of As_2O_3 to As_2S_3 using H_2S according to Equation 1 is thermodynamically feasible (Figure 3-3). In addition, the reaction must proceed fast enough to achieve complete conversion of As_2O_3 to As_2S_3 in a time that is practical for an industrial scale process. Therefore, the reaction must be kinetically favourable, but rates are not accounted for in the equilibrium geochemical modelling.

To further investigate the feasibility of heterogeneous As_2O_3 sulfidation, laboratory experiments were conducted which involved the injection of H_2S gas into a slurry of As_2O_3. A reaction product that resembled As_2S_3 (bright yellow) was generated, but analysis of the grains revealed that the reaction product was comprised of As_2O_3 grains that were thinly coated with As_2S_3; this indicated that the sulfidation reaction did not reach completion.

The results from these experiments demonstrate that the heterogeneous reaction of aqueous H_2S with slurried As_2O_3 powder results in passivation of the solid surfaces, a process which has been observed in various other reaction systems (Bi and Hayes, 2014; Peterson et al., 1997). At the onset of the sulfidation reaction, a monolayer of As_2S_3 forms on the surfaces of the As_2O_3 particles, and the rate of sulfidation is at

its peak (Figure 4-1). However, the rate begins to decrease as the coating of As_2S_3 grows thicker, and the reaction rate becomes limited by diffusion of H_2S through the coating of As_2S_3. This passivation results in incomplete sulfidation of the As_2O_3, and the reaction product is therefore not suitable for long-term disposal, necessitating an alterative approach to sulfidation.

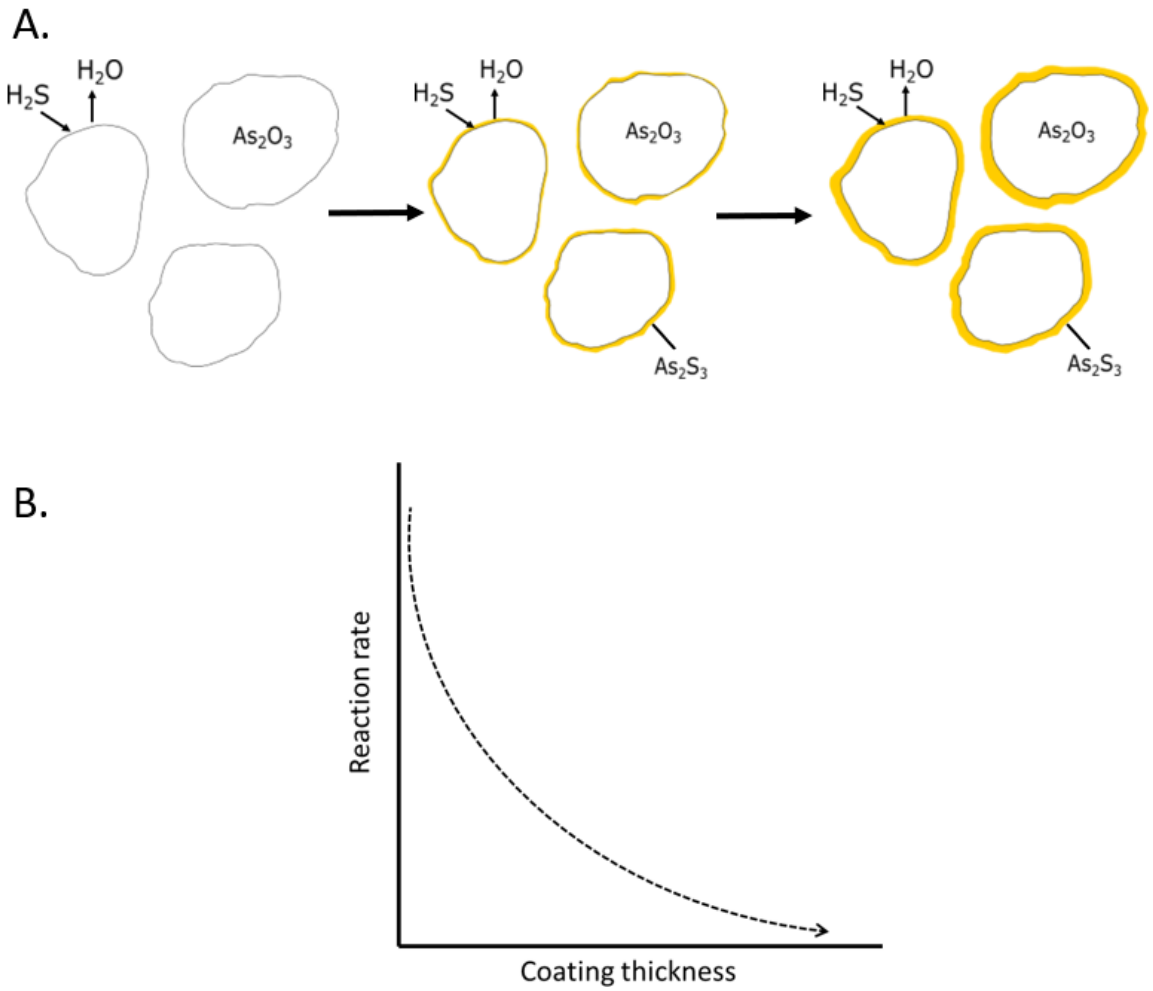

Figure 4-1: A. Illustration of As_2O_3 grain passivation due to formation of an As_2S_3 coating and B. Schematic of reaction rate trend with increasing coating thickness.

4.2. Homogeneous As_2O_3 sulfidation

The sulfidation of $H_3AsO_3^0$ and its hydrolysis products in solution to form As_2S_3 is rapid; this is known from previous research (Ostermeyer, 2021) and from qualitative experiments conducted in this study (Section 3.3.1). Therefore, recognizing that the dissolution of As_2O_3 is the limiting step toward complete transformation to As_2S_3 via a homogeneous reaction, the focus of the work transitioned to investigating the

most efficient method of dissolving the As_2O_3 in the Giant Mine waste. The two dissolution methods investigated were 1) dissolution of As_2O_3 in Na_2S at elevated pH, and 2) dissolution of As_2O_3 at elevated temperature.

4.2.1. Dissolution of As_2O_3 in sodium sulfide at high pH

The solubility of As_2O_3 increases with increasing pH (Zhang et al., 2014) and is known to readily dissolve in Na_2S solutions (Anderson et al. 2014; Lane et al., 2016). Sodium sulfide is a possible candidate for this method because the solution has a high pH and provides a sulfide source. An estimate of the quantity of Na_2S required to execute the dissolution of As_2O_3, and precipitation of As_2S_3 [Equation 8] is provided below.

$$6HCl_{(aq)} + 3Na_2S_{(aq)} + As_2O_{3\,(s)} \rightarrow 6NaCl_{(aq)} + As_2S_{3\,(s)} + 3H_2O_{(l)} \quad [8]$$

Previous work (SGS Lakefield Research, 2004) has determined that much of the Giant Mine dust is comprised of ≈ 60 wt. % arsenic (or ≈ 79 wt. % As_2O_3) (Table 1-2), which is used as a starting point for the calculation.

$$mass\ of\ As_2O_3 = percentage\ of\ As_2O_3 \times mass\ of\ Giant\ Mine\ dust$$
$$= 0.79 \times 237\,000\ tonnes$$
$$= 187\,000\ tonnes$$
$$= 1.87 \times 10^{11} g$$
$$moles\ of\ Na_sS\ required = \left(\frac{mass\ of\ As_2O_3}{molar\ mass\ of\ As_2O_3}\right) \times molar\ conversion$$
$$= \left(\frac{1.87 \times 10^{11} g}{197.841 g/mol}\right) \times 3$$
$$= 2.84 \times 10^9\ moles\ Na_sS$$

Stoichiometrically, 2.84 x 10^9 moles of Na_2S is estimated to execute Equation 8 to dissolve the As_2O_3.

Sodium sulfide solutions have a high pH; following As_2O_3 dissolution, the solution must therefore be acidified to a target pH (<5.5; Floroiu, 2004), where As_2S_3 precipitation is favourable. The quantity of acid

required to titrate Na_2S to a pH of 5.5 was calculated from the results of the PHREEQC simulation presented in Section 3.3.2. The simulation indicates that 1.95 moles of HCl are required per mole of Na_2S to titrate the solution to a pH of 5.5. At this ratio, if 2.84 x 10^9 moles of Na_2S are required to dissolve As_2O_3, approximately 5.53 x 10^9 moles of HCl are required to acidify the solution to a pH of 5.5. With the knowledge that concentrated (37%) HCl contains 12 moles HCl/L, then 5.53 x 10^9 moles of HCl translate to 4.61 x 10^8 L of concentrated HCl.

According to the website Tankmart International, a typical chemical tanker, capable of transporting acidic liquid products, has a capacity of approximately 34 000 L, necessitating greater than 13 000 tankers to transport 7.68 x 10^8 L of acid. The requirement of such a large quantity of acid introduces significant cost as well as health, safety, and transport risks to the remedial method. An alternative method was therefore pursued, focusing on dissolution of As_2O_3 in water at elevated temperature.

4.2.2. Dissolution of As_2O_3 at elevated temperature

With the understanding that heterogeneous sulfidation reactions lead to passivation of surfaces, it became clear that dissolution of As_2O_3 was necessary prior to sulfidation with a homogeneous aqueous reaction. Any process that might be designed to dissolve the As_2O_3 prior to sulfidation would benefit by maximizing the solubility because that would result in lower feed-water requirements and lower wastewater treatment requirements. Similarly, it would be advantageous to maximize the dissolution rate in order to increase the throughput and diminish the overall time to treat all of the waste. Optimization of the solubility and dissolution rates may also result in energy savings.

Results of previous research and experiments conducted in this study, indicate that the solubility of As_2O_3 increases systematically with temperature (CANMET, 2000; Pokrovski et al., 1996). The data from this study are superimposed on those from previous work in Figure 4-2: Solubility of As2O3 measured in this study, compared to previous measurements expressed in g As2O3/kg of water and moles of As/kg of water., demonstrating a consistent trend above 100 °C. This corroboration is valuable because it indicates that the

novel method used – visual observation of complete dissolution with a video camera in the microwave system – provides reliable solubility data.

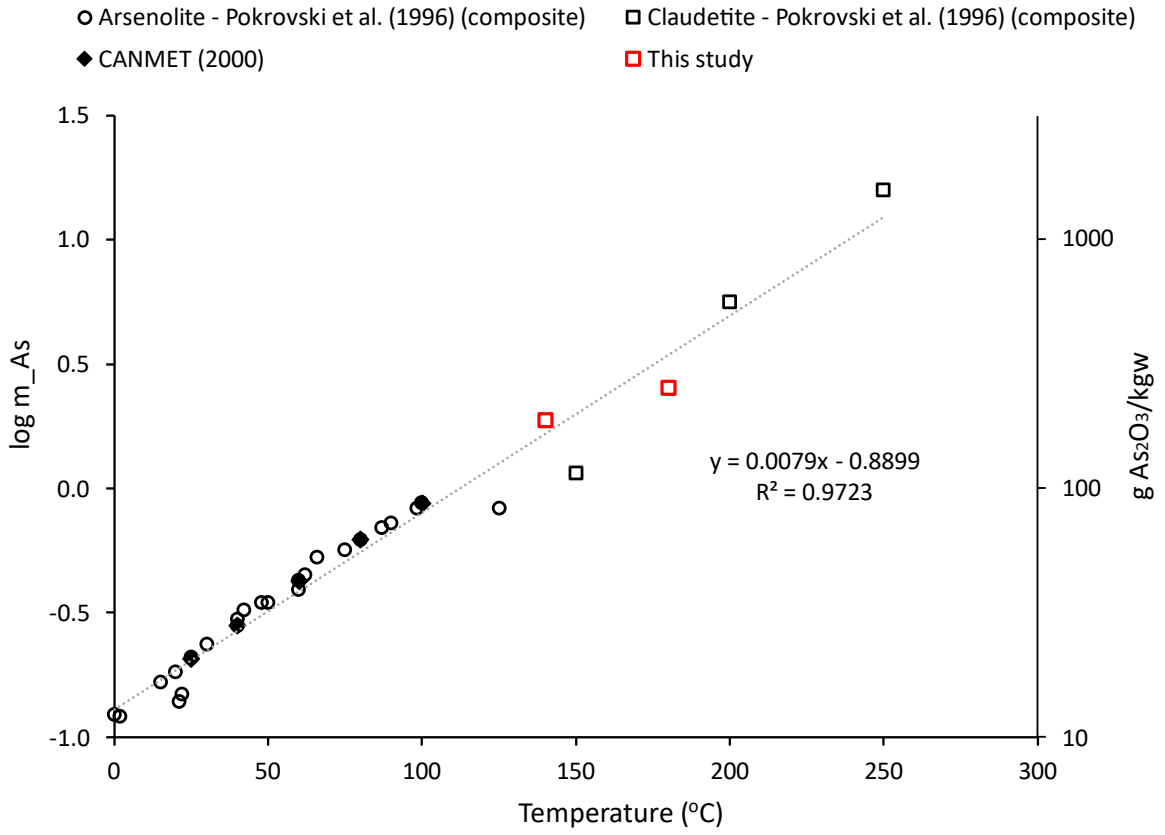

Figure 4-2: Solubility of As_2O_3 measured in this study, compared to previous measurements expressed in g As_2O_3/kg of water and moles of As/kg of water.

The initial dissolution rate of As_2O_3 was rapid at both 140 °C and 180 °C, where ≥ 90 % of the As_2O_3 dissolved within 5 minutes at 140°C and 4 minutes at 180 °C (Figure 3-11 and Figure 3-12). Key observations can be made from the dissolution rates determined both in this study and by CANMET (2000) at 60 °C (Figure 3-10). The dissolution rate increases systematically with increasing temperature (Figure 3-14), and at any given temperature the rate decreased with increasing time (Figure 3-13). A decrease in reaction rate with increasing As_2O_3 concentration is expected because the system is approaching equilibrium (Figure 3-11 and Figure 3-12). Uncertainties in the measured dissolution rates exist due to operational constraints of the microwave heating system. There is a ramp-up period during the approach to the target temperature (Figure 2-4) and a significant fraction of the As_2O_3 powder in the vessel is expected

to dissolve during the ramp up period. However, the time reported for complete dissolution refers only to the time at the target temperature. This has no effect on the solubility determinations, but given that some fraction of the total reaction occurs during the temperature ramp up period, there is a systematic overestimation of the reaction rate at the target temperature. The rates might best be described as apparent reaction rates.

Reports of kinetic reaction-rate constants for heterogeneous aqueous – solid reactions generally include measurements of solid surface area because rates are known to be a function of exposed surface area (Lasaga, 1998; Lengke and Tempel, 2001). Enquiries were made with several labs at uOttawa to obtain specific surface-area measurements for the reagent-grade As_2O_3, but it was not possible. The very rapid rates of As_2O_3 dissolution observed in these experiments demonstrate that the initial surface area degrades rapidly; to the point that it would be difficult to account for the effect of solid surface area on the rates. However, it is very unlikely that loss of solid surface area is a significant contributor to the observed decreases in dissolution rates as the reactions approached solubility equilibrium.

Both the dissolution rate and solubility of As_2O_3 were determined using visual determinations of the time to complete dissolution of As_2O_3 powder during heating in the microwave. Visual determination of As_2O_3 dissolution was utilized because the microwave vessel could not be opened above 100 ^oC and must be allowed to cool prior to sampling. Allowing the sample to cool would cause reprecipitation of As_2O_3 and would introduce systematic error in solubility measurements as documented in Section 3.3.6. While effective in eliminating the cooling-related source of error, the visual method is subject to error because reagent-grade As_2O_3 is white, and it can be difficult to discern the time-to-dissolution against the white interior of the microwave. In order to minimize this source of error, the microwave cavity was lined with black PTFE to increase the contrast between the powder and the background.

4.3. Dissolution of As_2O_3 in the Giant Mine dust

When conducting dissolution experiments with the Giant Mine sample B233-P9, there was a persistent undissolved residue that appeared to decrease slightly in mass with increasing extraction time (10 min – 30

min). The concentrations of As, Sb, and Fe in the undissolved residues did not vary (within error) with extraction time or temperature (Figures 3-17, 3-18, and 3-19). The rapid dissolution of As_2O_3 at elevated temperatures (Section 4.2.2) suggests that virtually all the As_2O_3 in the Giant Mine dust likely dissolved in less than 10 minutes.

4.3.1. Composition of undissolved Giant Mine sample B233-P9 residue

The residual As that remains following high-temperature extraction of the As_2O_3 is present primarily in two forms; i) As associated with Fe-oxide and oxyhydroxide phases and ii) small amounts of recalcitrant As_2O_3, in some cases in an As_2O_3-Sb_2O_3 solid solution (e.g. Figure 3-22 and Figure 3-23).

While minor, the presence of As_2O_3 in the residue is important because it provides insight into the efficiency of high-temperature extraction as a method toward stabilization of the Giant Mine As_2O_3 waste.

There are several possible explanations for the persistence of As_2O_3 grains:

1. Precipitation of As_2O_3 during the cooling stage of the microwave extraction cycle,
2. Elevated Sb_2O_3 concentration in solid solution with the As_2O_3 reduces the solubility relative to pure As_2O_3, and
3. Passivation of mixed As-Sb grains as selective dissolution of the As_2O_3 component leads to enrichment of Sb_2O_3 at the grain margins, or by the oxidation of As(III) at the surface followed by accumulation of a low-solubility As(V) phase.

If significant As_2O_3 reprecipitation did occur upon cooling of sample B233-P9, an increase in measured As concentrations would be expected in the residues from the higher-temperature extractions that have correspondingly longer cooling times. Visible As_2O_3 phases would also likely be apparent in the residue under investigation with SEM-EDS, particularly as overgrowths on other phases. The absence of both these features suggests that As_2O_3 reprecipitation upon cooling did not contribute significantly to the persistence of As in the residue of sample B233-P9.

The fine fraction of the B233-P9 residue contained a small amount of isolated As_2O_3 grains (Figure 3-20 to Figure 3-24). The As_2O_3 dissolution rate data show that ≥ 90 % of As_2O_3 should be dissolved in approximately 5 and 4 minutes, respectively, at 140 °C and 180 °C. All isolated As_2O_3 grains should therefore have dissolved in the time frame of the B233-P9 dissolution experiment (Section 3.4.3), in which heating times ranged from 10 min to 30 min.

Studies by both Poirier (2004) and CANMET (2000) determined that Sb_2O_3 is present in solid solution with some of the As_2O_3 crystals in the Giant Mine dust. For example, Poirier (2004) reported that some of the finer As_2O_3 grains (<10 µm) in sample B233-P9 contained up to 0.86 wt.% Sb_2O_3, and Sb_2O_3 concentrations as high as 30.1 wt.% were noted in samples from other storage chambers. The solubility of Sb_2O_3 was measured by CANMET (2000) and it is low relative to As_2O_3 (<10 mg/L at 25 ^oC and 55 mg/L at 95 ^oC), indicating that the presence of Sb_2O_3 as a solid solution end member would decrease the solubility of the $(Sb,As)_2O_3$ phase. The solubility decrease would be expected to evolve over time as As_2O_3 is preferentially dissolved, leaving Sb_2O_3 to accumulate at the grain surface and form a passivating barrier to further dissolution.

The incongruent dissolution of As_2O_3 within the solid solution could be further understood with information on the concentration and distribution of Sb_2O_3 within the individual grains. An attempt was made to further analyze the grains with electron microprobe, to acquire a more precise chemical analysis than can be provided with the SEM. However, irregular surfaces on the grains compromised the precision and accuracy of the results and the spatial resolution of the analyses was not sufficient to identify Sb_2O_3 zonation within the As_2O_3 grains.

Previous work conducted by CANMET (2000) and SRK (2004) found that the Giant Mine dust contains As-bearing hematite, and samples from the B233-P9 storage chamber were reported to have higher total hematite concentrations than others (Table 1-3; Poirier, 2004). Poirier (2004) reported that hematite grains within the Giant Mine dust (sample B233-P9) contain an average of 8.50 wt.% As. Much of the As that persists in the residue may be present in phases such as hematite, which is known to be a stable phase under

the conditions at which extraction experiments were carried out (e.g. Gordon Smith & Kidd, 1949; Zhao et al., 2019).

5. Conclusions

This research focused on determining a practical and effective method to transform As_2O_3 to a less soluble form, with a focus on As_2S_3, a low-solubility compound that could be safely disposed of deep in the mine to eliminate long-term risk to human health and the environment. The first approach was to investigate the heterogeneous sulfidation reaction between aqueous H_2S and an As_2O_3 slurry, but results demonstrated the formation of a thin coating of As_2S_3, passivating the surface of the As_2O_3 grains. The passivation slowed the reaction to the point that it would be impractical as a remedial method for the As_2O_3-rich dust at the Giant Mine.

Dissolution of As_2O_3 in high-pH Na_2S solutions was explored, followed by acidification of the solution to precipitate As_2S_3. This approach was also deemed impractical because of the risk involved with transporting large quantities of acid and other dangerous reagents to Yellowknife, and the likelihood that it would generate large volumes of water requiring treatment.

The research moved to pursue the potential for dissolution of As_2O_3 in pure water at elevated temperature, followed by sulfidation using H_2S, which is rapid when the As (III) is in an aqueous phase. This method would have the benefits of minimizing transportation of dangerous reagents and generation of highly saline waste waters. The research contributed to previously published data showing an increase in the solubility of As_2O_3 with increasing temperature (185.7 g As_2O_3/kg water at 140^{o}C and 250.6 g As_2O_3/kg water at 180 ^{o}C), as well as an increase in apparent dissolution rate; at each temperature, $\geq$ 90 % of the As_2O_3 was dissolved in minutes (5 minutes at 140 ^{o}C and 4 minutes at 180 ^{o}C).

Extraction experiments using pure water to dissolve As_2O_3 in the Giant Mine dust (Sb and Fe-rich sample B233-P9) at temperatures ranging from 140 ^{o}C to 200 ^{o}C consistently dissolved approximately 80 wt. % of the As, and virtually all of the As_2O_3, yielding a residue weighing approximately 40 wt.% of the initial

sample mass. Geochemical and mineralogical characterization shows that the residual As appears to be hosted in mixed low-solubility Fe-oxide and silicate phases, and in solid solution with Sb_2O_3.

References

Anderson, E., & Story, L (1923). Studies of certain physical properties of arsenic trioxide in water solution. Journal of American Chemical Society, 45, 1102-1105.

Anderson, C.G., Twidwell, L.G., Robins, R.G, & Mills, K.D. (2014). Arsenic Hydrometallurgy; Fundamentals, Technology, and Applications. Conference of Metallurgists Proceedings ISBN: 978-1-926872-24-7.

Baes, C.F., & Mesmer, R.E (1976). The hydrolysis of cations. New York: Wiley.

Bi, Y. and Hayes, K.F. (2014). Surface Passivation Limited UO_2 Oxidative Dissolution in the Presence of FeS. Environmental Science & Technology. 48 (22), 13402–13411.

Casado, J., Lopez-Quintela, M.A., and Lorenzo-Barral, F.M. The initial rate method in chemical kinetics: Evaluation and experimental illustration. Journal of Chemical Education., 63 (5), 450.

CANMET Mining and Mineral Sciences Laboratories (CANMET). (2000). Recovery and purification of arsenic oxide - Giant Mine, CANMET Project No. 601902.

Clark, I. D. (2001). Giant Mine Water Quality Data Interpretation. DIAND Contract No. 00-0055, Hull, Québec.

Cohen, Sidney. "Cost of cleaning up Yellowknife's Giant Mine now pegged at $4.38B, up from $1B". CBC News, 10 November 2022, https://www.cbc.ca/news/canada/north/giant-mine-remediation-cost-4-billion-1.6647952. Accessed 11 November, 2022.

Eary, L. E. (1992). The solubility of amorphous As_2S_3 from 25 to 90^{o}C. Geochimica and Cosmochimica Acta, 56, 2267 - 2280.

Floroiu, R. M., Davis, A. P., & Torrents, A. (2004). Kinetics and Mechanism of As_2S_3(am) Dissolution under N_2. Environmental Science & Technology, 38, 1031-1037.

Gordon Smith, F., & Kidd, D.J. (1949). Hematite-Goethite relations in neutral and alkaline solutions under pressure. University of Toronto, Canada.

Grenthe, I., Stumm., W., Laaksuharju, M., Nilsson, A.-C., Wikberg., P. (1992). Redox potentials and redox reactions in deep groundwater systems. Chemical Geology, 98, 131-150.

Jamieson, H. E. (2014). The Legacy of Arsenic Contamination from Mining and Processing Refractory Gold Ore at Giant Mine, Yellowknife, Northwest Territories, Canada. Reviews in Mineralogy & Geochemistry, 79, 533-551. doi:http://dx.doi.org/10.2138/rmg.2014.79.12

Lane, D.J., Cook, N.J., Grano, K.E. (2016). Selective leaching of penalty elements from copper concentrates: A review. Minerals Engineering. 98, 110-121.

Lasaga, A.C. (1998). Kinetic Theory in Earth Sciences. Princeton University Press.

Lichtner, P.C., & Waber, N. (1992). Redox front geochemistry and weathering: theory with application to the Osamu Utsumi uranium mine, Poços de Caldas, Brazil., Journal of Geochemical Exploration. 45, 1-3.

Linke, W.F. (1958). Solubilities of inorganic and metal-organic compounds, 4th ed. (pp. 234-240). Washington: American Chemical Society.

Lengke, M. F., & Tempel, R. N. (2001). Kinetic rates of amorphous As_2S_3 oxidation at 25 to 40°C and initial pH of 7.3 to 9.4. Geochimica et Cosmochimica Acta, 65(14), 2241 - 2255.

Mirazimi, S. M. (2020). Kinetics and mechanisms of arsenic release from amorphous and crystalline arsenic trisulfide. Vancouver: University of British Columbia.

Mironova, G.D., Zotov, A.V., Gul'ko, N.I (1984). Determination of the solubility of orpiment in acid solutions at 25-150°C. Geochemistry International. 21, 53-59.

Nordstrom, D. K., & Archer, D. G. (2002). Arsenic thermodynamic data and environmental geochemistry. In A. W. Stollenwerk, Arsenic in Ground Water (1-25). Boston: Kluwer Academic Publishers.

O'Day, P. (2006). The chemistry and mineralogy of arsenic. Elements, 2, 77-83.

Ostermeyer, P., Bonin, L., Folens, K., Verbruggen, F., Garcia-Timermans, C., Verbeken, K.,Rabaey, K., Hennebel, T. (2021). Effect of speciation and composition on the kinetics and precipitation of. Journal of Hazardous Materials, 409, 124418.

Parkhurst, D.L., Appelo, C.A.J. (2013) Description of input and examples for PHREEQC (Version 3). A computer program for speciation, batch-reaction, one-dimensional transport, and inverse geochem ical calculations. U.S. Geological Survey Techniques and Methods, (Book 6, Chap. A43, 497 p.) U.S. Geological Survey.

Peterson, M.L., White, A.F., Brown., G.E., Parks, G.A. (1997). Surface passivation of magnetite by reaction with aqueous Cr(VI): XAFS and TEM results. Environmental Science & Technology, 31 (5), 1573 – 1576.

Plumlee, G., & Morman, S. (2011). Mine wastes and human health. Elements, 7, 399-404.

Poirier, G. A mineralogical investigation of arsenic trioxide (As_2O_3) rick dust from the Giant Mine, Yellowknife, NWT. (2004). Prepared for SRK Consulting Ltd., LR-10750-001 - Final Report; in Appendix C of SRK (2004).

Pokrovski, G., Gout, R., Schott, J., Zotov, A., & Harrichoury, J.C. (1996). Thermodynamic properties and stoichiometry of As (III) hydroxide complexes at hydrothermal conditions. Geochimica et Cosmochimica Acta, 60(5), 737-749.

SENES Consultants Limited. (2002). Tier 2 risk assessment for management of arsenic trioxide dust, Giant Mine. Richmond Hill, ON.

SGS Lakefield Research Limited (2004). An investigation into the characterization of various arsenic trioxide dust samples from Giant Yellowknife Mine, prepared for SRK Consulting Ltd., LR-10750-001 - Final Report; in Appendix C of SRK (2004).

Singer, P. C., & Stumm, W. (1970). Acidic Mine Drainage: The Rate-Determining Step. Science, 167 (3921), 1121-1123.

SRK Consulting Inc. (SRK). (2004). Arsenic Trioxide Chamber Drilling and Testing Program. Supporting Document D1 of SRK and SENES Consulting Ltd. (2007).

SRK Consulting Inc. (SRK) (2002a). Final Report – Arsenic Trioxide Management Alternatives, prepared for Department of Indian and Northern Affairs Canada (INAC), 1CI001.10 Final Report.

SRK Consulting Inc. (SRK) (2002b). Supporting Document 2: Giant Mine hydrogeology studies – Supporting Document 2 to SRK (2002a).

SRK Consulting Inc. (SRK) and SENES Consulting Ltd. (SENES) (2007). Giant Mine remediation plan. Prepared for Department of Indian and Northern Affairs Canada (INAC).

Stranski, I.N., Plieth, K., Zoll, I (1958). Uber die Auflosung, die Loslichkeit und die Umwandlung der beiden Arsenik Modifikationen in Wasser und w&igen Losungen. Zeit. Electrochem. 62, 366-372.

Tankmart International. “Chemical Tank Trailer TC-407/DOT-407, TC-412/DOT-412”. https://www.tankmart.com/chemical-tank-trailers-for-sale.php.

Webster, J. (1990). The solubility of As_2S_3 and speciation of As in dilute and sulfide-bearing fluids at 25 and 90^{o}C. Geochimica et Cosmochimica Acta, 54, 1009-1017.

Wilkin, R.T., Wallschläger, D., Ford, R.G. (2003) Speciation of arsenic in sulfidic waters. Geochemical Transactions. 4,1-7.

Zhang, H., Yao, Q., Shao, LM. (2014) Recovery of Arsenic Trioxide from a Sludge-Like Waste by Alkaline Leaching and Acid Precipitation. Waste and Biomass Valorization, 5, 255–263.

Zhao, J., Brugger, J., Pring., A. (2019) Mechanism and kinetics of hydrothermal replacement of magnetite by hematite. Geoscience Frontiers, 10, 29-41.

Appendix A: Giant Mine Dust Geochemical Composition

Table 1: Bulk Chemical Analyses of Giant Mine Dust (SGS Lakefield Research, 2004)

Element (mg/kg)	C212-2 140-168	C212-2 168-189	B233-P9	B235-P13	Bag House	B208-1 Comp	B214-1 Comp	B212-4 Comp
Ag	1	6	38	9	20	4	9	6
Al	9300	6700	19000	7700	20000	4300	12000	7300
Ba	25	16	44	24	47	16	30	25
Be	0.1	0.1	0.1	0.1	0.1	0.25	0.25	0.25
Ca	6800	2300	9300	2900	9200	2300	5300	3400
Cd	12.5	12.5	12.5	12.5	12.5	4	4	4
Co	22	28	110	28	57	12.5	43	26
Cr	30	23	71	20	48	16	36	22
Cu	130	230	810	240	340	100	230	160
Fe	23000	21000	150000	20000	55000	18000	42000	25000
K	2600	1900	5200	2000	5000	1200	3600	2200
Mg	5500	500	5900	2900	6800	1600	3600	2200
Mn	170	88	300	100	250	74	130	85
Na	270	230	960	600	970	230	560	370
Ni	42	53	230	48	100	40	83	50
Pb	240	550	4300	440	1300	470	1200	810
Sb	2100	3600	18000	3700	8200	11000	16000	17000
Sr	8.1	5.7	14	5.8	16	3.2	44808	6
Ti	840	510	2000	610	1400	160	330	310
V	39	26	73	30	67	18	44	28
Y	0.9	0.9	2.1	1	1.8	0.7	1.6	1
Zn	220	250	2100	290	510	300	640	420
As (%)	62.7	66.33	39.5	66	51	66.5	57.8	60.2

Table 2: Solid phase near-total metal concentrations of Giant Mine B233-P9 sample obtained from coarse aggregates (n=10) and fine material (n=5)

Sample Type	Al	As	Ca	Cu	Fe	K	Mg	Na	Pb	Sb	Zn	S
Coarse (mg/kg)	6326	3.826×10^5	9184	630.9	8.711×10^4	1095	5210	570.9	3838	1.385×10^4	1621	-
	7443	4.490×10^5	10500	702.7	1.033×10^5	1261	6055	632.2	4395	1.562×10^4	1842	-
	6656	4.318×10^5	9795	649.6	8.666×10^4	1140	5595	557.1	3833	1.462×10^4	1644	-
	6119	3.454×10^5	8445	565.0	8.560×10^4	1029	4858	527.1	3538	1.270×10^4	1537	-
	6209	3.771×10^5	9673	615.3	8.898×10^4	1164	5336	673.4	3936	1.413×10^4	1609	-
	6561	4.137×10^5	10210	631.3	9.082×10^4	1123	5463	676.2	3842	1.316×10^4	1688	-
	6359	4.012×10^5	9395	640.5	8.770×10^4	1098	5416	693.4	3909	1.270×10^4	1632	-
	6083	4.230×10^5	8069	671.4	8.903×10^4	1181	5531	532.2	4087	1.680×10^4	1682	-
	6432	3.852×10^5	8772	610.2	8.641×10^4	1121	5224	499.5	3798	1.409×10^4	1587	-
	6881	4.288×10^5	10380	692.2	9.600×10^4	1301	5968	605.2	4287	1.663×10^4	1740	-
Fines (mg/kg)	5807	4.129×10^5	6413	515.6	9.118×10^4	179.2	4417	245.2	3894	1.303×10^4	1490	1.065×10^4
	6340	4.341×10^5	6945	499.1	9.659×10^4	188.3	4480	208.8	4146	1.306×10^4	1683	1.064×10^4
	6141	4.708×10^5	6710	524.0	9.321×10^4	198.1	4528	221.5	4208	1.386×10^4	1672	1.121×10^4
	6084	4.500×10^5	6655	489.7	8.766×10^4	186.4	4265	222.9	4134	1.270×10^4	1565	1.031×10^4
	6343	4.532×10^5	6777	477.6	9.401×10^4	186.5	4462	192.2	4156	1.272×10^4	1673	1.064×10^4
Summary Statistics												
Mean (mg/kg)	6386	4.173×10^5	8528	594.3	9.095×10^4	830.2	5121	470.5	4000	1.398×10^4	1644	1.069×10^4
Standard Deviation (mg/kg)	379.1	3.287×10^4	1446	73.69	4730	458.6	562.5	186.7	217.6	1343	82.20	291.2
Relative Standard Deviation (%)	5.937	7.878	16.96	12.40	5.201	55.24	10.99	39.68	5.441	9.610	4.999	2.724
Maximum (mg/kg)	7443	4.708×10^5	10500	702.7	1.033×10^5	1301	6055	693.4	4395	1.680×10^4	1842	1.121×10^4
Minimum (mg/kg)	5807	3.454 X 105	6413	477.6	8.560×10^4	179.2	4265	192.2	3538	1.270×10^4	1490	1.031×10^4

Table 3: Initial versus undissolved residue B233-P9 sample masses

Temperature	Time	Initial Sample	Undissolved Residue	Residual Mass Fraction
^{O}C	Minutes	g	g	wt. %
140	10	0.2409	0.0989	41.05
140	20	0.2618	0.1068	40.79
140	30	0.2336	0.1057	45.25
160	10	0.2197	0.0935	42.56
160	20	0.2313	0.0975	42.15
160	30	0.2346	0.0955	40.71
180	10	0.2671	0.1158	43.35
180	20	0.2291	0.0928	40.51
180	30	0.2614	0.1034	39.56
200	10	0.2432	0.1038	42.68
200	20	0.2794	0.1152	41.23
200	30	0.2878	0.118	41.00

Table 4: Solid phase concentrations in B233-P9 undissolved residues (mg/kg)

Reaction Temperature	Reaction Time	Al	As	Ca	Cu	Fe	K	Mg	Na	Pb	Sb	Zn
^{O}C	Minutes	mg/kg										
140	10	*$1.37x10^4$*	*$2.00\ x10^5$*	*$1.09\ x10^4$*	*1310*	*$1.92\ x10^5$*	*302.4*	*1879*	*427.1*	*9030*	*$2.72x10^4$*	*2901*
140	10	*$1.36x10^4$*	*$1.99x10^5$*	*$1.08\ x10^4$*	*1289*	*$1.92x10^5$*	*299.5*	*1862*	*424.9*	*8918*	*$2.69\ x10^4$*	*2906*
140	10	*$1.35x10^4$*	*$1.97x10^5$*	*$1.07\ x10^4$*	*1287*	*$1.91Ex10^5$*	*299.4*	*1847*	*401.7*	*8863*	*$2.67x10^4$*	*2881*
140*	10*	$1.36x10^4$	$1.99x10^5$	$1.08x10^4$	1295	$1.92x10^5$	300.4	1863	417.9	8937	$2.69x10^4$	2896
140	20	$1.389x10^4$	$1.851x10^5$	$1.093x10^4$	1182	$1.859x10^5$	303.7	1831	367.1	9600	$2.786x10^4$	2775
140	30	$1.351x10^4$	$2.009x10^5$	$1.067x10^4$	1152	$1.956x10^5$	283.2	2078	288.1	8818	$2.667x10^4$	2741
160	10	$1.33x10^4$	$1.88x10^5$	$1.09x10^4$	1134	$2.00x10^5$	276.6	2102	316.0	8990	$2.65x10^4$	2883
160	20	$1.40x10^4$	$1.95x10^5$	$1.06x10^4$	1194	$1.98x10^5$	314.3	2297	316.6	9112	$2.64x10^4$	2836
160	30	$1.44x10^4$	$1.90x10^5$	$1.07x10^4$	1266	$2.00x10^5$	289.5	2035	282.6	9558	$2.91x10^4$	2985
180	10	$1.391x10^4$	$1.998x10^5$	$1.105x10^4$	1222	$2.047x10^5$	293.3	2346	272.4	9204	$2.635x10^4$	3065
180	20	$1.42x10^4$	$1.99x10^5$	$1.11x10^4$	1198	$2.08x10^5$	329.0	2144	209.9	9492	$2.82x10^4$	3064
180	30	$1.479x10^4$	$2.042x10^5$	$1.056x10^4$	1213	$2.155x10^5$	292.5	2254	171.4	9770	$2.819x10^4$	3132
200	10	$1.348x10^4$	$2.130x10^5$	$1.071x10^4$	1144	$2.063x10^5$	277.7	2262	237.4	9207	$2.711x10^4$	3129
200	20	$1.373x10^4$	$2.062x10^5$	$1.035x10^4$	1252	$2.076x10^5$	303.7	2211	238.2	9473	$2.739x10^4$	3330
200	30	$1.362x10^4$	$2.140x10^5$	$9.633x10^3$	1210	$2.079x10^5$	269.1	2398	165.3	9320	$2.798x10^4$	3260

*Average of instrumental triplicate measurements (initial 3 rows)

Appendix B: PHREEQC Input Files

Input File 1: Initial conditions used to investigate the dissolution and precipitation reactions of an As_2O_3 slurry upon the addition of H_2S, in PHREEQC (Parkhurst and Appelo, 2013)

```
SOLUTION 1
   temp      10
   pH        6
   pe        4
   redox     pe
   units     mg/kgw
   density   1
   Ca        15
   Cl        27
   Fe        0.001
   K         0.5
   Mg        2
   Na        20
   Alkalinity 25
   -water    1 # kg
EQUILIBRIUM_PHASES 1
   Arsenolite 0 1
   Hematite  0 0.05
   As2S3(am) 0 0

REACTION 1
   H2S(g)     1
   0  0.25  0.5  0.75  1  1.25  1.5
   1.75  2  2.25  2.5  2.75  3  3.25  3.5
    3.75  4 moles

END
```

Input File 2: Initial conditions used to titrate a solution containing dissolved Na_2S with HCl, in PHREEQC (Parkhurst and Appelo, 2013)

```
SOLUTION 1
   temp      25
   redox     pe
   units     mol/kgw
   -water    1 # kg
Reaction 1
Na2S
0.1
Save Solution 1
END
USE Solution 1
Reaction
   HCl       1
   0.25 moles in 50 steps


END
```